

---

# FoR-SALE: Frame of Reference-guided Spatial Adjustment in LLM-based Diffusion Editing

---

Anonymous Author(s)

Affiliation

Address

email

## Abstract

Frame of Reference (FoR) is a fundamental concept in spatial reasoning that humans utilize to comprehend and describe space. With the rapid progress in Vision and Language models, the moment has come to integrate this long-overlooked dimension into these models. For example, in text-to-image (T2I) generation, even state-of-the-art models exhibit a significant performance gap when spatial descriptions are provided from perspectives other than the camera. To address this limitation, we propose **Frame of Reference-guided Spatial Adjustment in LLM-based Diffusion Editing** (FoR-SALE), an extension of the Self-correcting LLM-controlled Diffusion (SLD) framework for T2I. Specifically, we exploit visual processing modules, including object detection, depth detection, and orientation detection, to extract the necessary spatial cues for recognizing the possible perspectives. We use LLMs to convert all spatial expressions into a unified camera perspective before interpreting image layout. We exploit an image editing framework and introduce new latent operations to modify the facing direction and depth. We evaluate FoR-SALE on two benchmarks specifically designed to assess spatial understanding with FoR. Our framework improves the performance of state-of-the-art T2I models by up to 5.3% using only a single round of correction. Additionally, we provide a detailed analysis of the limitations of current T2I models from various perspectives, highlighting potential avenues for future research.

## 1 Introduction

Spatial understanding refers to the ability to comprehend the location of objects within a space. This ability is fundamental to human cognition and everyday tasks. A key component of this ability is dealing with the Frame of Reference (FoR) that defines the perspective from which spatial relations are interpreted. While extensively studied in cognitive linguistics Mou & McNamara (2002); Levinson (2003); Tenbrink (2011); Coventry et al. (2018), FoRs have received limited attention in AI models, particularly within Multimodal Large Language Models (MLLMs) Liu et al. (2023); Chen et al. (2024). Recent studies highlight substantial shortcomings in reasoning over FoR by MLLMs across multiple tasks, such as Visual Question AnsweringZhang et al. (2025b), Text-to-Image (T2I) generation Wang et al. (2025b), and text-based QA Prem Sri & Kordjamshidi



Figure 1: Examples of images generated by SOTA T2I models and the corresponding outputs after one round of correction using FoR-SALE.

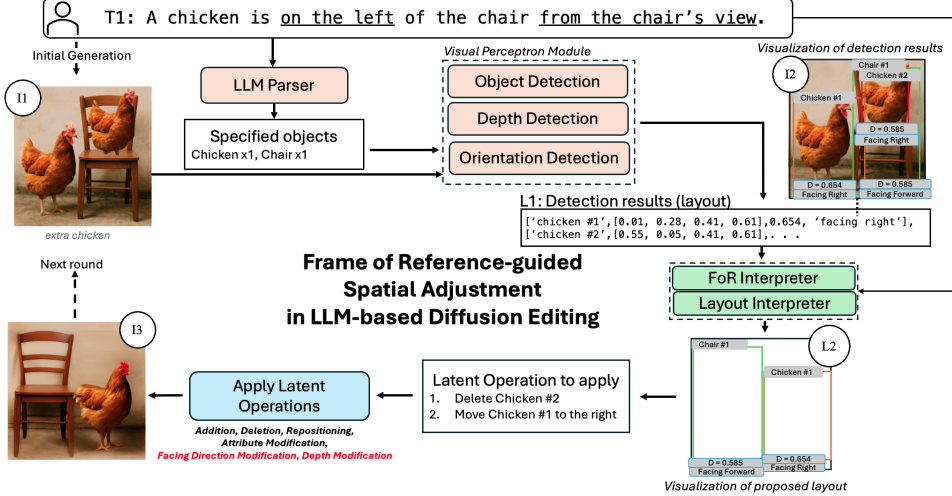


Figure 2: Overview of the FoR-SALE pipeline. It begins by extracting layout information from the initial image using an LLM Parser and a Visual Perception Module. This information is then passed through the FoR-Interpreter and Layout Interpreter to generate a revised layout. A sequence of latent operations is then derived by comparing the initial layout with revised layouts and applied to synthesize an updated image. The resulting image can undergo additional refinement rounds if needed.

(2025). One task that highlights a lack of reasoning over FoR is T2I generation. Wang et al. (2025b) and Premsri & Kordjamshidi (2025) show that diffusion models exhibit substantially lower spatial alignment when spatial expressions are described from non-camera perspectives. As illustrated in Figure 1, even SOTA T2I models—GPT-4oOpenAI (2025a) and FLUX.1Black Forest Labs (2025)—struggle to correctly generate images that reflect spatial relations described from non-camera perspectives. To address this issue, we propose the **Frame of Reference-guided Spatial Adjustment in LLM-based Diffusion Editing** (FoR-SALE) framework. Our approach builds upon the Self-correcting LLM-controlled Diffusion (SLD) pipeline Wu et al. (2024), which uses LLMs to validate prompts and generate suggested layouts for editing images through latent-space operations. However, the original SLD framework does not account for FoR, limiting its ability to handle spatial prompts grounded in perspectives other than the camera view. FoR-SALE extends this paradigm by explicitly modeling FoR and enabling spatial adjustment over diverse perspective conditions.

Figure 2 illustrates the FoR-SALE pipeline. The process begins with standard T2I generation, where a context ( $T_1$ ) is passed to a T2I module to produce an initial image ( $I_1$ ). Next, the LLM parser extracts the key object from the given context. Then, the key objects are passed to the Visual Perception Module to extract three types of visual information, that is, objects location, orientation, and depth. This extracted visual information ( $I_2$ ) is then converted into a textual format ( $L_1$ ). The input expression ( $T_1$ ) along with textual layout information ( $L_1$ ) is fed to the FoR Interpreter, which first identifies the frame of reference and converts the expression into the camera's perspective—a unified viewpoint. Subsequently, the Layout LLM is employed to generate a suggested layout ( $L_2$ ) in textual form that aligns with the updated spatial expression. Next, the suggested layout is compared with the visual detection outputs ( $L_1$ ) to identify mismatches, which are used to formulate self-correction operations, such as adjusting an object's facing direction or depth. These corrections are applied in the latent space during image synthesis using the Stable Diffusion model. Finally, a new image is generated from the corrected latent representation, ensuring consistency with the spatial configuration described in the input—particularly for the specified FoR. The resulting image ( $I_3$ ) can undergo additional refinement rounds if needed. We demonstrate the effectiveness of FoR-SALE using two benchmarks: FoR-LMD, a modification of the LMD Lian et al. (2024) benchmark that includes perspective, and FoREST Premsri & Kordjamshidi (2025), a benchmark that includes textual input for various FoR cases. We observed that our technique can improve images generated from SD-3.5-large, FLUX.1, and GPT-4o, SOTA models of T2I tasks, up to 5.30% improvement in a single correction round and 9.90% in three rounds. Moreover, we provide a thorough analysis to highlight

70 both the limitations of T2I models and LLMs used to suggest layouts from different perspectives.  
71 Our contribution<sup>1</sup> can be summarized as follows,  
72 **1.** We propose the first self-image correction framework that incorporates the notion of frame of  
73 reference (FoR) in T2I generation.  
74 **2.** We introduce novel editing operations within a self-correcting framework to handle various FoRs  
75 in generated images.  
76 **3.** We augment an existing benchmark to enable evaluation of FoR understanding in T2I models, and  
77 conduct a comprehensive evaluation across multiple T2I and self-correction frameworks. Our model  
78 achieves SOTA performance when applied to images generated by GPT-4o.

## 79 **2 Related Works**

80 **Frame of Reference in MLLMs.** Multiple benchmarks have been developed to evaluate the  
81 spatial understanding of MLLMs across various tasks Anderson et al. (2018); Mirzaee et al. (2021);  
82 Mirzaee & Kordjamshidi (2022); Shi et al. (2022); Cho et al. (2023). However, most of these  
83 benchmarks overlook the concept of FoR. Only a few recent benchmarks explicitly address FoR-  
84 related reasoning Liu et al. (2023); Chen et al. (2024); Zhang et al. (2025a); Wang et al. (2025a).  
85 For example, Liu et al. (2023) shows that training a vision-language model with text that includes  
86 FoR information can improve visual question answering (VQA). Wang et al. (2025a) introduces a  
87 comprehensive benchmark for spatial VQA that incorporates FoR examples, though FoR is not its  
88 central focus of evaluation. Three recent studies focus more directly on evaluating FoR understanding  
89 in MLLMs. First, Zhang et al. (2025b) assesses FoR handling in VQA settings and reveals substantial  
90 limitations, especially when reasoning goes beyond the default camera-centric view. Second, Prem Sri  
91 & Kordjamshidi (2025) investigates FoR reasoning in natural language prompts—both ambiguous and  
92 unambiguous—and finds persistent failures in both question answering and layout generation when  
93 the perspective diverges from the camera view. Third, Wang et al. (2025b) conducts a comprehensive  
94 evaluation of T2I models and finds that even SOTA models fail to preserve correct spatial relations  
95 when the context is not grounded in the camera’s perspective and includes 3D information such as  
96 orientation and distance. In this work, we extend this line of research by providing a new evaluation  
97 of T2I models based on their alignment with FoR-grounded spatial expressions. We also enhance the  
98 enhance the T2I models in comprehending varying FoR conditions.

99 **Spatial Alignment in T2I.** Several studies have sought to improve the spatial alignment of T2I  
100 models with user input. Early approaches introduced predefined spatial constraints—such as depth  
101 maps Zhang et al. (2023); Mo et al. (2024), object layouts Li et al. (2023), or attention maps Wang  
102 et al. (2024a); Pang et al. (2024)—to guide image generation. However, these often require manual  
103 configuration or model retraining to interpret the constraints. With advances in spatial reasoning from  
104 LLMs, recent work has leveraged them to generate spatial guidance automatically. For example, Cho  
105 et al. (2023) uses an LLM to generate initial layouts that guide diffusion models without additional  
106 training. More recent methods incorporate MLLMs to control 3D spatial arrangements by generating  
107 feedback used for reinforcement training of diffusion models Liu et al. (2025), train a T2I model using  
108 compositional questions derived from input prompts Sun et al. (2025), or produce action plans for  
109 sequential editing Wu et al. (2024); Goswami et al. (2024). While these methods are promising, they  
110 ignore the reasoning issues across FoR variations. In contrast, we explicitly address this limitation by  
111 extending the SLD framework Wu et al. (2024) to support editing under diverse FoRs.

## 112 **3 Methodology**

113 In this section, we explain our proposed FoR-SALE, an extension of the SLD framework Wu et al.  
114 (2024). An overview of the framework is illustrated in Figure 2. FoR-SALE follows the SLD  
115 framework, which consists of two main components: (1) LLM-driven visual perception and (2)  
116 LLM-controlled layout interpretation. However, we adapt the two components to accommodate  
117 more fine-grained perception and layout interpretation for recognizing FoR and correcting the image  
118 accordingly.

---

<sup>1</sup>Code will be publicly available upon acceptance.

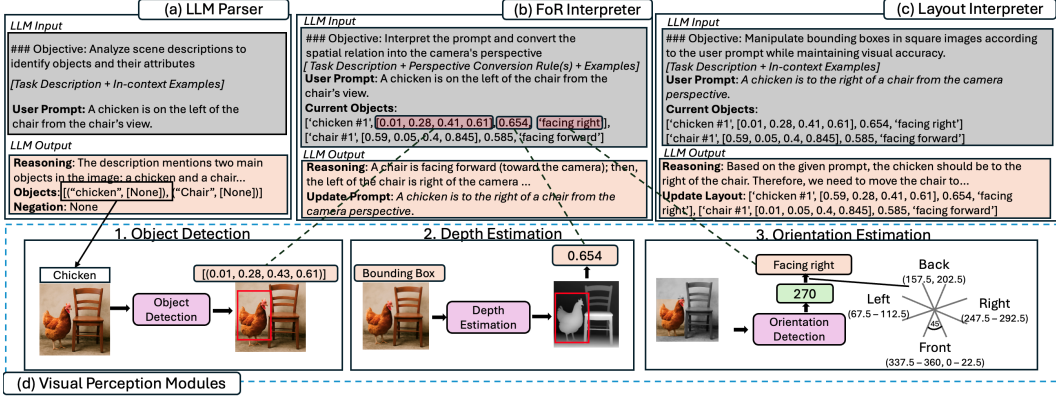


Figure 3: Example inputs and outputs from the LLM Parser, FoR Interpreter, Layout Interpreter, and Visual Perception Module. The LLM Parser output guides the Visual Perception Module in extracting object-specific information, including bounding boxes, orientation, and depth. This information is passed to the FoR Interpreter, which converts the spatial expression to the camera’s perspective. The Layout Interpreter then generates a suggested spatial layout based on the updated prompt.

### 119 3.1 LLM-driven Visual perception Module

120 The process begins with standard T2I generation, where a textual input is passed to a T2I model to  
 121 create an image. The FoR-SALE then proceeds by extracting necessary information from both the  
 122 spatial expression using an LLM parser and the generated image using a visual perception module.

#### 123 3.1.1 LLM parser

124 In this first step, we prompt an LLM to extract a list of key object mentions and their attributes from  
 125 the input text, denoted as  $L$ . To facilitate accurate extraction, we provide the LLM with textual  
 126 instructions and in-context examples. For example, given the spatial expression *A red chicken is on*  
 127 *the left of a chair from the chair’s view*. The output of LLM is  $L = \{("chicken", ["red"]), ("chair",$   
 128  $[\text{None}]\}$  where “red” is the attribute associated with the chicken, and “None” indicates that no specific  
 129 attribute is mentioned for the chair.

#### 130 3.1.2 Visual Perception Module

131 The obtained list  $L$  is fed into the visual perception module in the SLD framework with an open-  
 132 vocabulary object detection. In our FoR-SALE, we add new visual perception components to deal  
 133 with FoR. These include depth estimation and orientation detection. Figure 3 (d) illustrates this  
 134 module. The open-vocabulary object detector receives information in  $L$  with the following prompt  
 135 format “image of a/an [attribute] [object name]” and outputs bounding boxes, denoted as  $B$ . The  
 136 outputs are represented in the following list format,  $((\text{attribute}) (\text{object name}) (\#\text{object}$   
 137  $\text{ID}), [x, y, w, h])$  where  $(x, y)$  indicates the coordinates of the upper-left corner of the bounding  
 138 box from 0.0 to 1.0,  $w$  is its width, and  $h$  is its height. The object ID is a serial number assigned  
 139 uniquely to each detected object. Next, the depth estimation model is used to predict the depth map  
 140 of the image, denoted as  $D$ . To extract object-specific depth values, denoted as  $D_i$ , a segmentation  
 141 mask is applied using the bounding boxes from  $B$  and computes the average pixel depth within each  
 142 masked region using the following equation,  $D_i = \sum_j^R d_j / |R|$  where  $i$  is id of the object,  $R$  is the  
 143 mask region of the object, and  $d_j$  is depth at pixel  $j$ . The value of  $D_i$  ranges from 0 to 1. Finally, an  
 144 orientation detection model is invoked over the object segmentation to obtain the orientation angle  
 145 of the object. This angle is then converted into a facing direction, denoted as  $f_i$ . There are eight  
 146 facing direction categories:  $\text{orientation} = \{\text{ForwardLeft}, \text{Left}, \text{BackwardLeft}, \text{Back}, \text{BackwardRight},$   
 147  $\text{Right}, \text{ForwardRight}, \text{Front}\}$ . Each category spans a 45-degree range, starting from  $22.5^\circ$  to  $67.5^\circ$  for  
 148 ForwardLeft, and continuing in  $45^\circ$  intervals for the remaining orientation labels. We collect these  
 149 visual information about each object and obtain a new list with these detail in a new format, denoted  
 150  $V_L = \{((\text{attribute}) (\text{object name}) (\#\text{object ID}), [x, y, w, h], D_i, f_i)\}$ . An example of  
 151 representation can be found in Figure 2.

152 **3.2 LLM Controlled Diffusion**

153 After obtaining visual information ( $V_L$ ), two additional modules are employed to analyze and modify  
154 the image, that is, LLM-Interpreters and Image Correction.

155 **3.2.1 LLM-Interpreters**

156 This module analyzes  $V_L$  together with the input text  $T$  and proposes a revised layout, denoted as  
157  $\tilde{V}_L$  in the same format. The original SLD framework employs an LLM for layout interpretation.  
158 However, in FoR-SALE, we incorporate one additional LLM, that is, FoR interpreter. Figure 3 (b)  
159 and (c) illustrate these two LLMs.

160 **1) FoR-Interpreter.** Based on the findings of Zhang et al. (2025b), Prem Sri & Kordjamshidi (2025),  
161 and Wang et al. (2025b), MLLMs demonstrate significantly stronger performance when reasoning  
162 over spatial expressions described from the camera perspective. Motivated by this observation, we  
163 hypothesize that converting the perspective of the spatial expressions into a camera viewpoint can  
164 alleviate this issue. The input to FoR-Interpreter consists of the spatial text,  $T$ , and visual information  
165 of the generated image,  $V_L$ . The output is a spatial expression rewritten from the camera perspective,  
166 denoted as  $T'$ . If no spatial relation is present, the model returns the input text unchanged. We provide  
167 an in-context information scheme for the FoR-Interpreter to conduct this perspective conversion.  
168 In particular, we include spatial perspective conversion rules. A total of 32 rules are manually  
169 defined—one for each combination of the eight facing directions considered in the Visual Perception  
170 Module and four spatial relations (front, back, left, right). e.g., *if the object is facing left, the left side*  
171 *of the object is in front of the camera*. All rules are included in the Appendix. An example of the  
172 input and output is shown in Figure 3(b).

173 **2) Layout Interpreter.** After obtaining the spatial expression,  $T'$ , that follows the camera perspective,  
174 the second LLM uses  $T'$  and  $V_L$  as input to analyze the layout. The Layout-Interpreter LLM is  
175 prompted with manually crafted in-context examples to analyze whether the current layout aligns  
176 with the provided  $T'$ . If misalignment is detected, the LLM is instructed to propose a revised layout  
177  $\tilde{V}_L$  that satisfies the spatial description. An example of the input and output is shown in Figure 3(c).

178 **3.2.2 Image Correction**

179 In this step, we compare the current layout  $V_L$  with the proposed layout  $\tilde{V}_L$  using an exact matching  
180 process to detect the misalignment. If there is any misalignment between the two layouts, we  
181 create a sequence of editing operations to modify the image and align it with  $\tilde{V}_L$ . The original  
182 SLD framework includes four editing operations: Addition, Deletion, Reposition, and Attribute  
183 Modification. Our framework extends this set by introducing **two new operations for handling**  
184 **FoR**, that is, Facing Direction Modification and Depth Modification. Before applying any operation,  
185 backward diffusion Ho et al. (2020) is performed on the initial image to obtain its latent representation,  
186 which serves as the basis for all subsequent editing actions. After all editing actions are applied,  
187 Stable Diffusion is called to synthesize the final image.

188 **1) Addition.** Following the prior framework by Wu et al. (2024), this operation involves two main  
189 steps. First, it generates the target object within the designated bounding box area using base Stable  
190 Diffusion, and then generates the object’s segment using SAM Kirillov et al. (2023). Next, we  
191 perform a backward diffusion process with the base diffusion model over the generated object region  
192 to extract a new object latent representation. This object-specific latent representation is then merged  
193 into the latent space of the original image to complete the composition.

194 **2) Deletion.** The process first segments the object using SAM within its bounding box. The latent  
195 representation corresponding to the segmented region is then removed and replaced with Gaussian  
196 noise. This replacement allows the object’s region to be reconstructed during the final diffusion step.

197 **3) Reposition.** To preserve the object’s aspect ratio, this step begins by shifting and resizing the  
198 object from its original bounding box to the new target bounding box. After repositioning, SAM  
199 is used to do object segmentation. Then, a backward diffusion process is used to obtain the latent  
200 representation. This new representation is then integrated into the latent space of the original image at  
201 the updated location. To remove the object from the original position, we replace the corresponding  
202 latent region, identified via SAM at the original bounding box, with Gaussian noise before the final  
203 diffusion step.

Table 1: Accuracy of generated images across baseline models and editing methods, including FoR-SALE. Relative denotes camera-based spatial expression; Intrinsic uses another object’s perspective.

Method	FoR-LMD			FoREST			Overall Avg.
	Relative	Intrinsic	Average	Relative	Intrinsic	Average	
SD 3.5 - Large	63.75	24.72	42.60	18.11	11.11	15.00	28.80
+ 1-round GraPE	55.46	16.97	34.60	14.91	7.56	11.60	23.10
+ 1-round SLD	61.57	19.56	38.80	22.55	11.55	17.60	28.20
<b>+ 1-round FoR-SALE (Ours)</b>	<b>61.14</b>	<b>26.56</b>	<b>42.40</b>	<b>24.00</b>	<b>16.00</b>	<b>20.40</b>	<b>31.40</b>
+ 2-round FoR-SALE (Ours)	67.25	26.94	45.40	28.00	22.22	25.40	35.40
<b>+ 3-round FoR-SALE (Ours)</b>	<b>70.31</b>	<b>29.52</b>	<b>48.20</b>	<b>28.00</b>	<b>22.22</b>	<b>25.40</b>	<b>36.80</b>
FLUX.1	58.95	25.83	41.00	18.18	15.56	17.00	29.00
+ 1-round GraPE	54.15	18.08	34.60	17.45	11.56	14.80	24.70
+ 1-round SLD	63.32	25.09	42.60	24.72	12.00	19.00	30.80
<b>+ 1-round FoR-SALE (Ours)</b>	<b>65.07</b>	<b>27.67</b>	<b>44.80</b>	<b>25.09</b>	<b>22.22</b>	<b>23.80</b>	<b>34.30</b>
+ 2-round FoR-SALE (Ours)	67.68	<b>28.04</b>	<b>46.20</b>	30.18	29.78	30.00	38.10
<b>+ 3-round FoR-SALE (Ours)</b>	<b>69.43</b>	25.84	45.80	<b>32.72</b>	<b>31.11</b>	<b>32.00</b>	<b>38.90</b>
GPT-4o	<b>94.76</b>	24.35	56.60	<b>57.81</b>	35.56	47.80	52.20
+ 1-round GraPE	93.89	19.56	53.60	55.64	30.22	44.20	48.90
+ 1-round SLD	89.08	21.40	52.40	43.27	23.56	34.40	43.40
<b>+ 1-round FoR-SALE (Ours)</b>	93.01	35.42	61.80	54.18	37.33	46.60	54.20
+ 2-round FoR-SALE (Ours)	93.01	34.32	61.20	48.73	39.11	44.40	52.80
<b>+ 3-round FoR-SALE (Ours)</b>	91.26	<b>38.37</b>	<b>62.60</b>	53.81	<b>42.22</b>	<b>48.60</b>	<b>55.60</b>

204 **4) Attribute Modification.** To edit an object’s attribute, it begins by employing SAM to segment the  
 205 object region within its bounding box. An attribute modification diffusion model, e.g., DiffEdit Coua-  
 206 iron et al. (2023), is then called with a new prompt to modify the object’s attribute within the defined  
 207 region. For example, calling DiffEdit with the prompt “a red car” modifies the color of a car in the  
 208 specified region to red. After the attribute is edited, a backward diffusion process is performed to  
 209 extract the corresponding latent representation. This updated latent is then integrated into the image  
 210 latent space to complete the modification.

211 **5) Facing direction Modification.** This process is similar to an attribute modification. It begins by  
 212 using SAM to segment the object’s region. Then it invokes the DiffEdit with a prompt specifying  
 213 the desired facing direction to generate an image of the object with the new orientation. Next,  
 214 the base diffusion model is used to perform a backward diffusion process for obtaining the latent  
 215 representation of the reoriented object. Finally, this latent is integrated into the overall image latent  
 216 space to complete the modification.

217 **6) Depth Modification.** It begins by synthesizing the new depth of the given object using the  
 218 equation,  $d_{j'} = \min(1, \max(0, d_j - D_i + D_{i'}))$ , where  $d_j$ ,  $d_{j'}$  denote the original and updated  
 219 depth values of pixel  $j$ , respectively.  $D_i$  represents the current average depth of object  $i$  defined in  
 220 Section 3.1.2, and  $D_{i'}$  is the new target depth proposed by the LLM interpreter. Next, we shift and  
 221 resize the synthesized depth map of this object to the target bounding box. A diffusion model is  
 222 then called with ControlNet Zhang et al. (2023) to generate an object with the specified depth. After  
 223 generating a new object, the segmentation and backward diffusion are performed to obtain the latent  
 224 representation of the object at the new depth. Finally, this latent representation is integrated into the  
 225 image latent space to complete the modification.

## 226 4 Experiments

### 227 4.1 Datasets

228 **FoR-LMD.** We extend the LMD benchmark Lian et al. (2024), which is a synthetic dataset and was  
 229 designed to assess several reasoning skills that include spatial understanding. We augment the input  
 230 spatial expressions in LMD by adding explicit perspective cues to incorporate FoR information. The  
 231 LMD prompt template is:  $(obj_1)(R_1)$  and  $(obj_2)(R_2)$ , where  $obj_1$  and  $obj_2$  are objects, and  $R_1$ ,  $R_2$   
 232 are spatial relations. We modify it to:  $(obj_1)(R_1)(ref_1)$  and  $(obj_2)(R_2)(ref_2)$ , where  $ref_1$  and  
 233  $ref_2$  specify the reference perspective—camera view (relative), or object-centric view (intrinsic). To

Table 2: Accuracy of suggested layout and edited images from the corresponding layout under different Layout Interpreters using initial images generated from GPT4o.

Layout Interpreters	LLM-Layout Accuracy			Image Accuracy		
	Relative	Intrinsic	Average	Relative	Intrinsic	Average
o3	<b>99.40</b>	79.03	<b>89.30</b>	69.24	30.64	50.10
o4-mini	99.20	64.52	82.00	<b>74.40</b>	29.44	52.10
Qwen3	98.21	45.97	72.30	73.61	21.77	47.90
FoR-Interpreter(No-Rules) + Qwen3	95.23	54.03	74.80	69.84	24.80	47.50
FoR-Interpreter(Partial-Rules) + Qwen3	93.25	81.65	87.50	70.63	<b>39.52</b>	<b>55.20</b>
FoR-Interpreter(Full-Rules) + Qwen3	93.85	<b>84.48</b>	89.20	71.82	36.29	54.20

234 emphasize relations sensitive to perspective, we restrict  $R_1, R_2$  to left, right, front, back. This results  
 235 in 500 samples of spatial expression with explicit perspective.

236 **FoREST** Premsri & Kordjamshidi (2025) is a synthetic benchmark designed to evaluate the FoR  
 237 understanding in multimodal models with FoR annotation. We sample 500 spatial expressions from  
 238 the C-split of FoREST to match the size of FoR-LMD. Each prompt explicitly specifies the spatial  
 239 perspective and the facing direction of the reference object, which is not provided in FoR-LMD.

## 240 4.2 Evaluation Method

241 We adapted the proposed evaluation scheme in Wang et al. (2025b), which is shown to align with  
 242 human judgment. However, we modified some evaluation aspects, such as facing direction. In  
 243 detail, to evaluate the generated image, we call the Visual Perception Module to extract the bounding  
 244 boxes, depth, and orientations of key objects from an LLM parser as explained in Section 3.1. After  
 245 obtaining the visual information for all key objects, we verify that the number of objects matches the  
 246 given explanation in the text. We should note that in evaluated benchmarks, exactly one instance of  
 247 each object must be present in the image. If this counting condition does not match, the image is  
 248 considered incorrect. Next, we evaluate whether the detected orientation label matches the orientation  
 249 specified in the annotated data. Any misalignment results in the image being marked as incorrect.  
 250 Next, for the evaluation of the spatial relations, we consider the FoR annotation provided in the  
 251 context. If the FoR is not camera-centric (relative), we convert the spatial relation into the camera  
 252 perspective using the detected orientation of the reference object (relatum) by applying the same  
 253 procedure explained in FoR Interpreter. Finally, we use the pre-defined geometric specifications of  
 254 the spatial relations Huang et al. (2023); Cho et al. (2023); Wang et al. (2025b), assuming the camera  
 255 perspective, to assess the correctness of the spatial configuration.

## 256 4.3 Baseline Models

257 For baseline comparison, we select six T2I models: Stable Diffusion (SD) 1.5Rombach et al.  
 258 (2022), SD 2.1Rombach et al. (2022), SD 3.5-LargeStability AI (2024), GLIGENLi et al. (2023),  
 259 FLUX.1Black Forest Labs (2025), and GPT-4o-imageOpenAI (2025b). The number of Inference  
 260 Steps is set to 30 for SD3.5-Large, recommended by the original paper Stability AI (2024), while the  
 261 rest is set to 50. Other parameters are set to the default for all models. Given our focus on recent  
 262 models, results for older baselines—including SD 1.5, SD 2.1, and GLIGEN—are presented in the  
 263 Appendix. For comparison with editing frameworks that leverage LLMs to guide image modifications,  
 264 we include SLD and GraPE Goswami et al. (2024)—two self-correcting editing pipelines that achieve  
 265 SOTA results by using GPT4o as the LLM-Interpreter. All experiments were conducted on two  
 266 A6000 GPUs, totaling around 400 GPU hours.

## 267 4.4 FoR-SALE Implementation Detail

268 We select Qwen3-32B Qwen Team (2025) with reasoning enabled as the backbone LLM for all  
 269 LLM components used in the FoR-SALE pipeline. For the Visual Perception module, we employ  
 270 OWLv2 Minderer et al. (2024) for open-vocabulary object detection, DPT Ranftl et al. (2021) for  
 271 depth estimation, and OrientAnything Wang et al. (2024b) for orientation detection. We utilize SD  
 272 1.5 as the base diffusion model for creating objects and the final step of denoising the composed  
 273 latent space.

Table 3: Accuracy of image generated from FoR-SALE with exclude either facing or depth Modification and SLD using initial images generated from FLUX.1.

Method	Accuracy		
	Relative	Intrinsic	Average
SLD	42.26	19.15	30.80
FoR-SALE	43.25	25.20	34.30
- Facing Direction Modification	40.67	22.17	31.50
- Depth Modification	42.65	25.20	34.00

## 274 4.5 Results

275 **RQ1. Can the SOTA T2I models follow the FoR expressed in the text?** As can be seen in  
276 Table 1, the best-performing model, GPT-4o-image, achieves only 52.20% accuracy, highlighting the  
277 difficulty of T2I generation—even with only two objects in a spatial relation. While GPT-4o performs  
278 well on relative FoR in FoR-LMD (94.76%), its accuracy drops sharply to 24.35% on intrinsic FoR,  
279 revealing a substantial performance gap. This trend is consistent with findings from FoRESTMemsri  
280 & Kordjamshidi (2025) and GenSpaceWang et al. (2025b), which emphasize the challenges of FoR  
281 reasoning beyond camera perspective. Interestingly, GPT-4o’s advantage in relative FoR disappears  
282 in intrinsic settings, suggesting its improvements are largely limited to camera-based understanding.  
283 In the FoREST benchmark, which has explicit facing direction in the input, GPT-4o still maintains a  
284 relative lead—likely due to its better handling of facing direction. We also observe that GPT-4o may  
285 benefit from orientation cues in improving intrinsic FoR alignment. In contrast, other models fail to  
286 leverage such information and continue to struggle under both relative and intrinsic FoRs.

287 **RQ2. How effective is FoR-SALE framework in editing  
288 images to follow the FoR expressed in text?** To answer  
289 this question, we compare FoR-SALE with two existing  
290 auto-editing frameworks: SLD and GraPE. FoR-SALE  
291 generally outperforms both, except in the relative FoR  
292 setting of the FoR-LMD benchmark, where SLD slightly  
293 excels. We attribute this to the simplicity of camera per-  
294 spective contexts in that setting, which do not require FoR  
295 reasoning. However, FoR-SALE is still competitive with  
296 only a minor 0.40% accuracy drop. In contrast, for more  
297 challenging intrinsic FoR settings, FoR-SALE achieves  
298 substantial improvement, up to 5% after one round and  
299 15% after three rounds. Other frameworks consistently  
300 struggle in such cases. We also observe consistent over-  
301 all performance improvements with additional rounds of  
302 FoR-SALE. Figure 4 presents a detailed error analysis

303 comparing images from FLUX.1 with those edited by SLD and FoR-SALE. FoR-SALE shows clear  
304 improvements in left and right relations, which can often be corrected through 2D spatial adjustments.  
305 This improvement is expected when the layout interpreter accurately infers the FoR, which shows  
306 a positive impact of the FoR Interpreter. It also reduces many orientation errors, though correcting  
307 3D aspects such as depth and facing direction remains challenging, with a high error rate persisting  
308 in those categories. Performance on front and back relations shows limited improvement and, in  
309 some cases, worsens compared to SLD, which highlights the difficulty of 3D editing. We suspect that  
310 SLD’s apparent improvement in front/back errors does not lead to an overall performance increase, as  
311 it introduces new errors due to a lack of depth information. To evaluate this hypothesis, we provide a  
312 further analysis in the Appendix comparing the error on the front and back relations. It reveals that  
313 SLD’s front/back errors are reduced due to the generation of extra objects, which are later counted as  
314 multiple-object errors. Finally, we observe that multiple-object/missing object errors remain high for  
315 both models, indicating a limitation in current editing frameworks.

## 316 5 Ablation Study

317 **RQ3. How accurate do the LLMs perform Layout-Editing?** To address this question, we conduct  
318 an ablation study on the LLMs used for the Layout Interpreter, evaluating two SOTA reasoning

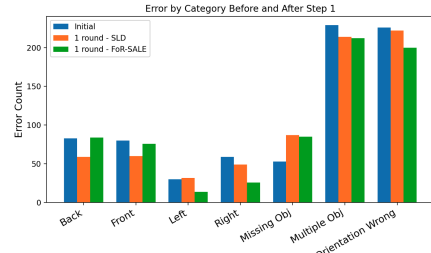


Figure 4: Error analysis of images generated by FLUX.1 (blue) and after one round of editing using SLD (orange) or FoR-SALE (green).

319 models: o3 and o4-mini OpenAI (2025a). We also examine three settings for the FoR Interpreter. (1)  
320 No-Rule, where no rules are provided. (2) Partial-Rules, which include only facing direction-related  
321 rules explicitly present in the input or detection results. (3) Full-Rules, which include all rules. We  
322 report accuracy using the evaluation protocol described in Section 4.2, measuring the quality of the  
323 LLM-generated layout and the accuracy of the final image produced after editing. Table 2 presents  
324 the results of this experiment. The accuracy of the LLM-generated layouts is significantly higher  
325 than that of the corresponding generated images, highlighting the challenge of correctly executing  
326 layout-guided edits. Despite this, a clear performance gap remains between relative (camera-centric)  
327 and intrinsic (non-camera) FoR—particularly for Qwen3 without the FoR Interpreter. We observe  
328 that incorporating the FoR Interpreter leads to noticeable performance improvements for Qwen3,  
329 especially in handling intrinsic FoR. Moreover, adding perspective conversion rules further enhances  
330 Qwen3’s ability to reason over intrinsic FoR. Notably, with these enhancements, Qwen3 outperforms  
331 o3 on intrinsic FoR, which presents the more challenging reasoning. Although the FoR Interpreter  
332 slightly reduces Qwen3’s layout accuracy in the relative case (by 5%), it yields a substantial +38.5%  
333 improvement on intrinsic FoR, affirming the overall effectiveness of this module. We also find that  
334 although o3 produces more accurate layouts than both o4-mini and our layout interpreter, it results in  
335 a lower final image accuracy. We hypothesize that this is due to o3’s generated layouts requiring a  
336 higher number of editing actions, making it more difficult for the editing framework. To evaluate  
337 this hypothesis, we analyze the distribution of editing actions required to align the image with the  
338 newly generated layout. Our analysis shows that o3’s layouts require, on average, more repositioning  
339 operations and a higher number of total actions than those generated by the other LLMs; the details  
340 are reported in the appendix.

341 **RQ4. How do the new editing actions help FoR-SALE?** To answer this question, we conduct an  
342 ablation study by disabling facing direction or depth modification in FoR-SALE, using initial images  
343 from FLUX.1. As shown in Table 3, removing facing direction modification reduces accuracy by  
344 2.8%, while removing depth modification leads to a 0.30% drop. Nevertheless, both of them are still  
345 better than the baseline. These results highlight the importance of both editing actions—especially  
346 facing direction—in improving spatial alignment. The limited impact of depth editing suggests it  
347 remains a challenge, and future work may focus on enhancing its effectiveness.

## 348 6 Conclusion

349 Given the limitations of current text-to-image (T2I) models in handling spatial relations across  
350 diverse frames of reference (FoR), we propose FoR-SALE—Frame of Reference-guided Spatial  
351 Adjustment in LLM-based Diffusion Editing—to address this challenge. Our framework extends  
352 the Self-correcting LLM-controlled Diffusion approach by introducing three key components: a  
353 comprehensive Visual Perception Module, a dedicated FoR Interpreter, and two new latent editing  
354 actions. FoR-SALE can be seamlessly integrated into various T2I models and effectively improves the  
355 spatial alignment of images initially generated by those models—achieving up to 5.30% improvement  
356 in a single correction round and 9.90% in 3 rounds. Using GPT-4o as the base generator, our method  
357 achieves SOTA performance on spatial expressions involving FoRs, particularly for intrinsic FoRs,  
358 which are especially challenging. These results demonstrate the robustness of reasoning over FoR of  
359 our proposed framework.

## 360 7 Limitations

361 While we identify shortcomings of existing Text-to-Image models, our intention is to highlight areas  
362 for improvement rather than to disparage prior work. Our analysis is constrained to a synthetic  
363 provides controlled conditions but may not fully capture real-world contexts. In addition, our study  
364 is limited to English, and does not account for linguistic or cultural variations in spatial expression.  
365 Extending this work to multiple languages may reveal important differences in frame-of-reference  
366 comprehension. Furthermore, the evaluation results of our experiments can vary depending on  
367 the choice of visual perception modules. We emphasize that these modules are used solely for  
368 comparative purposes and do not resolve the broader challenges of visual perception. Finally, our  
369 experiments require substantial GPU resources, which restricted the range of large language models  
370 we were able to test. These computational demands also pose accessibility challenges for researchers  
371 with limited resources.

372 **References**

373 Peter Anderson, Qi Wu, Damien Teney, Jake Bruce, Mark Johnson, Niko Sünderhauf, Ian Reid,  
374 Stephen Gould, and Anton van den Hengel. Vision-and-language navigation: Interpreting visually-  
375 grounded navigation instructions in real environments. In *Proceedings of the IEEE Conference on*  
376 *Computer Vision and Pattern Recognition (CVPR)*, 2018.

377 Black Forest Labs. Flux.1 kontext: Flow matching for in-context image generation and editing in  
378 latent space, 2025. URL <https://arxiv.org/abs/2506.15742>.

379 Boyuan Chen, Zhuo Xu, Sean Kirmani, Brian Ichter, Danny Driess, Pete Florence, Dorsa Sadigh,  
380 Leonidas Guibas, and Fei Xia. Spatialvlm: Endowing vision-language models with spatial  
381 reasoning capabilities, 2024. URL <https://arxiv.org/abs/2401.12168>.

382 Jaemin Cho, Abhay Zala, and Mohit Bansal. Visual programming for step-by-step text-to-image  
383 generation and evaluation. In *Thirty-seventh Conference on Neural Information Processing Systems*,  
384 2023. URL <https://openreview.net/forum?id=yhBFG9Y85R>.

385 Guillaume Couairon, Jakob Verbeek, Holger Schwenk, and Matthieu Cord. Diffedit: Diffusion-based  
386 semantic image editing with mask guidance. In *The Eleventh International Conference on Learning*  
387 *Representations*, 2023. URL <https://openreview.net/forum?id=3lge0p5o-M->.

388 Kenny R. Coventry, Elena Andonova, Thora Tenbrink, Harmen B. Gudde, and Paul E. Engelhardt.  
389 Cued by what we see and hear: Spatial reference frame use in language. *Frontiers in Psychology*,  
390 Volume 9 - 2018, 2018. ISSN 1664-1078. doi: 10.3389/fpsyg.2018.01287. URL <https://www.frontiersin.org/journals/psychology/articles/10.3389/fpsyg.2018.01287>.

392 Ashish Goswami, Satyam Kumar Modi, Santhosh Rishi Deshineni, Harman Singh, Prathosh A. P,  
393 and Parag Singla. Grape: A generate-plan-edit framework for compositional t2i synthesis, 2024.  
394 URL <https://arxiv.org/abs/2412.06089>.

395 Jonathan Ho, Ajay Jain, and Pieter Abbeel. Denoising diffusion probabilistic models.  
396 In *Advances in Neural Information Processing Systems (NeurIPS)*, volume 33,  
397 pp. 6840–6851, 2020. URL <https://proceedings.neurips.cc/paper/2020/file/4c5bcfec8584af0d967f1ab10179ca4b-Paper.pdf>.

399 Kaiyi Huang, Kaiyue Sun, Enze Xie, Zhenguo Li, and Xihui Liu. T2i-compbench: A comprehensive  
400 benchmark for open-world compositional text-to-image generation. *Advances in Neural*  
401 *Information Processing Systems*, 36:78723–78747, 2023.

402 Alexander Kirillov, Eric Mintun, Nikhila Ravi, Hanzi Mao, Chloe Rolland, Laura Gustafson, Tete  
403 Xiao, Spencer Whitehead, Alexander C. Berg, Wan-Yen Lo, Piotr Dollár, and Ross Girshick.  
404 Segment anything, 2023. URL <https://arxiv.org/abs/2304.02643>.

405 Stephen C. Levinson. *Space in Language and Cognition: Explorations in Cognitive Diversity*.  
406 Language Culture and Cognition. Cambridge University Press, 2003.

407 Yuheng Li, Haotian Liu, Qingyang Wu, Fangzhou Mu, Jianwei Yang, Jianfeng Gao, Chunyuan Li,  
408 and Yong Jae Lee. Gligen: Open-set grounded text-to-image generation. *CVPR*, 2023.

409 Long Lian, Boyi Li, Adam Yala, and Trevor Darrell. LLM-grounded diffusion: Enhancing prompt  
410 understanding of text-to-image diffusion models with large language models. *Transactions on*  
411 *Machine Learning Research*, 2024. ISSN 2835-8856. URL <https://openreview.net/forum?id=hFALpTb4fR>. Featured Certification.

413 Fangyu Liu, Guy Edward Toh Emerson, and Nigel Collier. Visual spatial reasoning. *Transactions of*  
414 *the Association for Computational Linguistics*, 2023.

415 Zheyuan Liu, Munan Ning, Qihui Zhang, Shuo Yang, Zhongrui Wang, Yiwei Yang, Xianzhe Xu,  
416 Yibing Song, Weihua Chen, Fan Wang, and Li Yuan. Cot-lized diffusion: Let's reinforce t2i  
417 generation step-by-step, 2025. URL <https://arxiv.org/abs/2507.04451>.

418 Matthias Minderer, Alexey Gritsenko, and Neil Houlsby. Scaling open-vocabulary object detection,  
419 2024. URL <https://arxiv.org/abs/2306.09683>.

420 Roshanak Mirzaee and Parisa Kordjamshidi. Transfer learning with synthetic corpora for spatial role  
 421 labeling and reasoning. In Yoav Goldberg, Zornitsa Kozareva, and Yue Zhang (eds.), *Proceedings*  
 422 *of the 2022 Conference on Empirical Methods in Natural Language Processing*, pp. 6148–6165,  
 423 Abu Dhabi, United Arab Emirates, December 2022. Association for Computational Linguistics. doi:  
 424 10.18653/v1/2022.emnlp-main.413. URL <https://aclanthology.org/2022.emnlp-main.413/>.

426 Roshanak Mirzaee, Hossein Rajaby Faghihi, Qiang Ning, and Parisa Kordjamshidi. SPARTQA:  
 427 A textual question answering benchmark for spatial reasoning. In Kristina Toutanova, Anna  
 428 Rumshisky, Luke Zettlemoyer, Dilek Hakkani-Tur, Iz Beltagy, Steven Bethard, Ryan Cotterell,  
 429 Tanmoy Chakraborty, and Yichao Zhou (eds.), *Proceedings of the 2021 Conference of the North*  
 430 *American Chapter of the Association for Computational Linguistics: Human Language Technologies*, pp. 4582–4598, Online, June 2021. Association for Computational Linguistics. doi: 10.18653/  
 431 v1/2021.naacl-main.364. URL <https://aclanthology.org/2021.naacl-main.364/>.

433 Sicheng Mo, Fangzhou Mu, Kuan Heng Lin, Yanli Liu, Bochen Guan, Yin Li, and Bolei Zhou.  
 434 Freecontrol: Training-free spatial control of any text-to-image diffusion model with any condition.  
 435 In *Proceedings of the IEEE/CVF Conference on Computer Vision and Pattern Recognition (CVPR)*,  
 436 pp. 7465–7475, June 2024.

437 Weimin Mou and Timothy P McNamara. Intrinsic frames of reference in spatial memory. *J Exp*  
 438 *Psychol Learn Mem Cogn*, 28(1):162–170, January 2002.

439 OpenAI. Addendum to gpt-4o system card: Native image generation. Technical Report Na-  
 440 tive\_Image\_Generation\_System\_Card, OpenAI, San Francisco, CA, March 2025a. Available  
 441 at: [https://cdn.openai.com/11998be9-5319-4302-bfbf-1167e093f1fb/Native\\_Image\\_Generation\\_System\\_Card.pdf](https://cdn.openai.com/11998be9-5319-4302-bfbf-1167e093f1fb/Native_Image_Generation_System_Card.pdf).

443 OpenAI. Gptimage1 (gpt-4o image generation). <https://openai.com/index/introducing-4o-image-generation/>, 2025b. Integrated image generation mode of  
 444 GPT-4o, replacing DALL-E3 in ChatGPT as of March25,2025.

446 Lianyu Pang, Jian Yin, Baoquan Zhao, Feize Wu, Fu Lee Wang, Qing Li, and Xudong Mao.  
 447 Attndreambooth: Towards text-aligned personalized text-to-image generation. In *The Thirty-  
 448 eighth Annual Conference on Neural Information Processing Systems*, 2024. URL <https://openreview.net/forum?id=4bINoegDcm>.

450 Tanawan Premsri and Parisa Kordjamshidi. Forest: Frame of reference evaluation in spatial reasoning  
 451 tasks, 2025. URL <https://arxiv.org/abs/2502.17775>.

452 Qwen Team. Qwen3 technical report, 2025. URL <https://arxiv.org/abs/2505.09388>.

453 René Ranftl, Alexey Bochkovskiy, and Vladlen Koltun. Vision transformers for dense prediction.  
 454 *ArXiv preprint*, 2021.

455 Robin Rombach, Andreas Blattmann, Dominik Lorenz, Patrick Esser, and Björn Ommer. High-  
 456 resolution image synthesis with latent diffusion models. In *Proceedings of the IEEE/CVF Confer-  
 457 ence on Computer Vision and Pattern Recognition (CVPR)*, pp. 10684–10695, June 2022.

458 Zhengxiang Shi, Qiang Zhang, and Aldo Lipani. Stepgame: A new benchmark for robust multi-  
 459 hop spatial reasoning in texts. In *Proceedings of the AAAI Conference on Artificial Intelligence*,  
 460 volume 36, pp. 11321–11329, Jun. 2022. doi: 10.1609/aaai.v36i10.21383. URL <https://ojs.aaai.org/index.php/AAAI/article/view/21383>.

462 Stability AI. Stable diffusion 3.5 large. <https://huggingface.co/stabilityai/stable-diffusion-3.5-large>, 2024. Multimodal Diffusion Transformer (MMDiT)  
 463 text-to-image model with 8.1billion parameters; released under Stability AI Community License.

465 Jiao Sun, Deqing Fu, Yushi Hu, Su Wang, Royi Rassin, Da-Cheng Juan, Dana Alon, Charles  
 466 Herrmann, Sjoerd Van Steenkiste, Ranjay Krishna, and Cyrus Rashtchian. DreamSync: Aligning  
 467 text-to-image generation with image understanding feedback. In Luis Chiruzzo, Alan Ritter, and  
 468 Lu Wang (eds.), *Proceedings of the 2025 Conference of the Nations of the Americas Chapter of  
 469 the Association for Computational Linguistics: Human Language Technologies (Volume 1: Long*

470      *Papers*), pp. 5920–5945, Albuquerque, New Mexico, April 2025. Association for Computational  
 471      Linguistics. ISBN 979-8-89176-189-6. doi: 10.18653/v1/2025.naacl-long.304. URL <https://aclanthology.org/2025.naacl-long.304/>.

473      Thora Tenbrink. Reference frames of space and time in language. *Journal of Pragmatics*, 43(3):  
 474      704–722, 2011. ISSN 0378-2166. doi: <https://doi.org/10.1016/j.pragma.2010.06.020>. URL <https://www.sciencedirect.com/science/article/pii/S037821661000192X>. The Language  
 475      of Space and Time.

477      Ruichen Wang, Zekang Chen, Chen Chen, Jian Ma, Haonan Lu, and Xiaodong Lin. Compositional  
 478      text-to-image synthesis with attention map control of diffusion models. *Proceedings of the AAAI  
 479      Conference on Artificial Intelligence*, 38(6):5544–5552, 2024a. doi: 10.1609/aaai.v38i6.28364.

480      Xingrui Wang, Wufei Ma, Tiezheng Zhang, Celso M de Melo, Jieneng Chen, and Alan Yuille.  
 481      Spatial457: A diagnostic benchmark for 6d spatial reasoning of large multimodal models. *CVPR*,  
 482      2025a. URL <https://arxiv.org/abs/2502.08636>.

483      Zehan Wang, Ziang Zhang, Tianyu Pang, Chao Du, Hengshuang Zhao, and Zhou Zhao. Orient any-  
 484      thing: Learning robust object orientation estimation from rendering 3d models. *arXiv:2412.18605*,  
 485      2024b.

486      Zehan Wang, Jiayang Xu, Ziang Zhang, Tianyu Pang, Chao Du, Hengshuang Zhao, and Zhou Zhao.  
 487      Genspace: Benchmarking spatially-aware image generation, 2025b. URL <https://arxiv.org/abs/2505.24870>.

489      Tsung-Han Wu, Long Lian, Joseph E. Gonzalez, Boyi Li, and Trevor Darrell. Self-correcting llm-  
 490      controlled diffusion models. In *Proceedings of the IEEE/CVF Conference on Computer Vision and*  
 491      *Pattern Recognition (CVPR)*, pp. 6327–6336, June 2024.

492      Lvmin Zhang, Anyi Rao, and Maneesh Agrawala. Adding conditional control to text-to-image  
 493      diffusion models, 2023.

494      Yue Zhang, Zhiyang Xu, Ying Shen, Parisa Kordjamshidi, and Lifu Huang. SPARTUN3d: Situated  
 495      spatial understanding of 3d world in large language model. In *The Thirteenth International  
 496      Conference on Learning Representations*, 2025a. URL <https://openreview.net/forum?id=FGMkSL8NR0>.

498      Zheyuan Zhang, Fengyuan Hu, Jayjun Lee, Freda Shi, Parisa Kordjamshidi, Joyce Chai, and Ziqiao  
 499      Ma. Do vision-language models represent space and how? evaluating spatial frame of reference  
 500      under ambiguities. In *The Thirteenth International Conference on Learning Representations*,  
 501      2025b. URL <https://openreview.net/forum?id=84pDoCD41H>.

## 502      A FoR-SALE Implementation Details

503      Random seed are set into an arbitrary number, 78 in all of our experiments, for reproducible results.

### 504      A.1 LLM Parser

505      For the implementation of the LLM Parser, we employ Qwen3-32B with reasoning generation  
 506      (thinking tokens) disabled to enable faster inference, given the simplicity of the task. The temperature  
 507      is set to 0 for reproducible results, and the maximum token limit is 8196. Listing 2 in Section G  
 508      provides the complete prompt and examples used for this LLM Parser.

### 509      A.2 FoR Interpreter

510      We select Qwen3-32B with reasoning generation (thinking tokens) enabled for the FoR Interpreter, as  
 511      this component requires reasoning over the provided rules. To ensure reproducibility, the temperature  
 512      is set to 0, and the maximum token limit is 8196. Listing 4 in Section G presents the complete prompt  
 513      and examples used for the FoR Interpreter.

514 **A.3 Layout Interpreter**

515 Similar to the FoR Interpreter, we use Qwen3-32B with reasoning generation (thinking tokens)  
516 enabled for this LLM component. For the ablation study, we also evaluate two additional LLMs via  
517 the OpenAI API: o3 (model name: o3-2025-04-16) and GPT-o4-mini, both from OpenAI. To ensure  
518 reproducibility, the temperature is set to 0, and the maximum token limit is 8196. This configuration  
519 is applied consistently across all LLMs used in the Layout Interpreter. The prompt for this Layout  
520 Interpreter is in Listing 4 in Section G.

521 **A.4 Visual Perception Module**

522 For the implementation of the Visual Perception Module, we employ three components including  
523 object detection, depth estimation, and orientation detection as mentioned in the main paper. For  
524 open-vocabulary object detection, we use OWLViT2, with the model ID *google/owlv2-base-patch16-ensemble*. For depth estimation, we select DPT, using the model ID *Intel/dpt-large*. Finally, for  
525 526 orientation detection, we employ OrientAnything, with ViT-Large as the base model. The model  
527 528 weights are loaded from the checkpoint *croplargeEX2/dino\_weight.pt*, as provided in the official  
GitHub repository.

529 **B Evaluation Functions**

530 There are a total of four evaluation functions used to evaluate the generated image. The visual details  
531 are represented in the following format: ((attribute) (object name) (#object ID), [x, y,  
532 w, h],  $D_i$ ,  $f_i$ ) where  $(x, y)$  indicates the coordinates of the upper-left corner of the bounding box  
533 from 0.0 to 1.0,  $w$  is its width,  $h$  is its height,  $D_i$  is depth from 0.0 to 1.0 which 1.0 is indicate nearest  
534 to the camera, and  $f_i$  is facing direction label. Each comparison involves two objects, denoted as  $obj_1$   
535 and  $obj_2$ . Before performing the comparison, we compute the center of each object's bounding box,  
536 denoted by  $(c_x, c_y)$ , where  $c_x = x + w/2$  and  $c_y = y + h/2$ . The procedure for each comparison is  
537 described below.

- **Left.** We determine whether the center of  $obj_1$  is to the left of  $obj_2$  by checking whether  $c_x$   
of  $obj_1$  is less then  $c_x$  of  $obj_2$ . The condition is defined as,

$$c_x^{obj_1} < c_x^{obj_2}$$

538 .

- **Right.** We determine whether the center of  $obj_1$  is to the right of  $obj_2$  by checking whether  
539  $c_x$  of  $obj_1$  is greater then  $c_x$  of  $obj_2$ . The condition is defined as,

$$c_x^{obj_1} > c_x^{obj_2}$$

- **Front.** We determine whether  $obj_1$  is front of  $obj_2$  by comparing  $D_1$  (depth of  $obj_1$ ) with  
540  $D_2$  (depth of  $obj_2$ ) . The condition is defined as,

$$D_1 > D_2$$

- **Back.** Similar to front relation, we compare  $D_1$  with  $D_2$  using following condition,

$$D_1 < D_2$$

539 **C Baseline Models Parameters**

540 **C.1 Stable Diffusion (SD)**

541 For baselines using SD1.5 and SD2.1, we set the number of inference steps to 50, while keeping all  
542 other parameters at their default values. The model ID for SD1.5 is *sd-legacy/stable-diffusion-v1-5*,  
543 and for SD2.1, it is *stabilityai/stable-diffusion-2-1*. The baseline using SD3.5-Large employs the  
544 model ID *stabilityai/stable-diffusion-3.5-large*, with the number of inference steps set to 30; all other  
545 parameters remain unchanged.

Method	FoR-LMD			FoREST			Overall Avg.
	Relative	Intrinsic	Average	Relative	Intrinsic	Average	
SD 1.5	12.66	11.80	12.20	7.63	4.00	6.00	9.10
SD 2.1	13.97	10.33	12.00	5.09	7.11	6.00	9.00
Qwen3 + GLIGEN	58.52	21.40	38.40	2.54	1.33	2.00	20.20

Table 4: Accuracy of generated images across pioneer diffusion models and editing methods.

## 546 C.2 GLIGEN

547 We use Qwen3 to generate the initial layout for the GLIGEN baseline. The prompt used for layout  
 548 generation is shown in Listing 1. For the GLIGEN model, we use the model ID *masterful/glichen-1-4-generation-text-box*. We also provide facing direction information when generating images with  
 549 GLIGEN by augmenting the object names with the corresponding facing directions extracted from  
 550 the layout generated by Qwen3. The number of inference steps is set to 50, while all other parameters  
 551 remain unchanged.

## 553 C.3 FLUX.1

554 For generating images with FLUX.1 baseline, we employ the pipeline with model id *black-forest-labs/FLUX.1-dev*. The guidance scale is set to 3.5, following the recommended value. The image  
 555 resolution is 1024×1024, and the number of inference steps is set to 50. Other parameters are set as  
 556 default.

## 558 C.4 GPT4o-image

559 We utilize the OpenAI API to generate images for the GPT-4o baseline, employing the model ID *gpt-image-1*. The background setting is set to auto, and the image resolution is configured to 1024×1024.  
 560 All other parameters are left at their default values. The cost for generating one image is around  
 561 \$0.01 – \$0.02.

## 563 D Additional Result on Text-to-Image (T2I) baselines

### 564 D.1 Additional results of pioneer T2I

565 We provide additional results for early T2I models, including SD1.5, SD2.1, and GLIGEN, using  
 566 layouts generated by Qwen3 in Table 4.  
 567 All models perform significantly worse than  
 568 the SOTA baselines discussed in the main re-  
 569 sults—particularly SD1.5 and SD2.1, which  
 570 achieve less than 10% accuracy. While GLIGEN  
 571 shows more acceptable performance on the FoR-  
 572 LMD benchmark, it performs poorly when orien-  
 573 tation requirements are introduced, as in context  
 574 of the FoREST benchmark. GLIGEN’s accuracy  
 575 drops to just 2%, indicating a lack of under-  
 576 standing of object-level attributes—especially facing  
 577 direction—even when this information is explic-  
 578 itly provided during generation.

### 580 D.2 Image 581 generation error of different baselines

582 Figure 5 illustrates the error distribution for images generated by SD3.5-Large, FLUX.1, and GPT-4o.  
 583 We observe notable differences among these models. Note that, while SD3.5-Large and FLUX.1 are  
 584 diffusion-based T2I models, GPT-4o is a unified generative model trained on multimodal input-output  
 585 tasks. GPT-4o exhibits significantly fewer missing or additional key objects, indicating stronger object

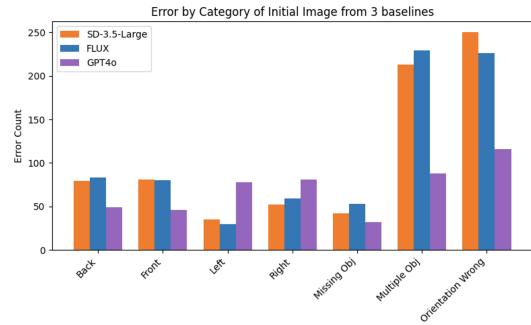


Figure 5: Error analysis of image generated by SD-3.5-Large, FLUX.1, and GPT4o,

Layout Interpreter	Add	Remove	Attribute	Reposition (R)	Facing	Depth (D)	D + R	# Actions
o3	3.60	10.63	0.00	49.82	15.95	10.45	9.55	1110
o4-mini	4.98	11.92	0.00	39.85	20.64	18.98	3.75	906
Qwen3	3.66	10.47	0.00	36.65	16.86	25.65	6.70	955
FoR-I(No-Rules)+Qwen3	3.81	9.18	0.00	42.47	13.40	26.91	4.23	970
FoR-I(Partial-Rules)+Qwen3	3.33	8.22	0.00	41.78	10.76	31.12	4.79	1022
FoR-I(Full-Rules)+Qwen3	3.40	6.90	0.00	43.25	11.95	29.74	4.86	1029

Table 5: The percentage of editing action required for editing both FoR-LMD and FoREST using the initial image from GPT4o based on different Layout Interpreters. FoR-I stands for FoR-Interpreter. Attribute refers to Attribute Modification, Depth refers to Depth Modification, and Facing refers to Facing Direction Modification.

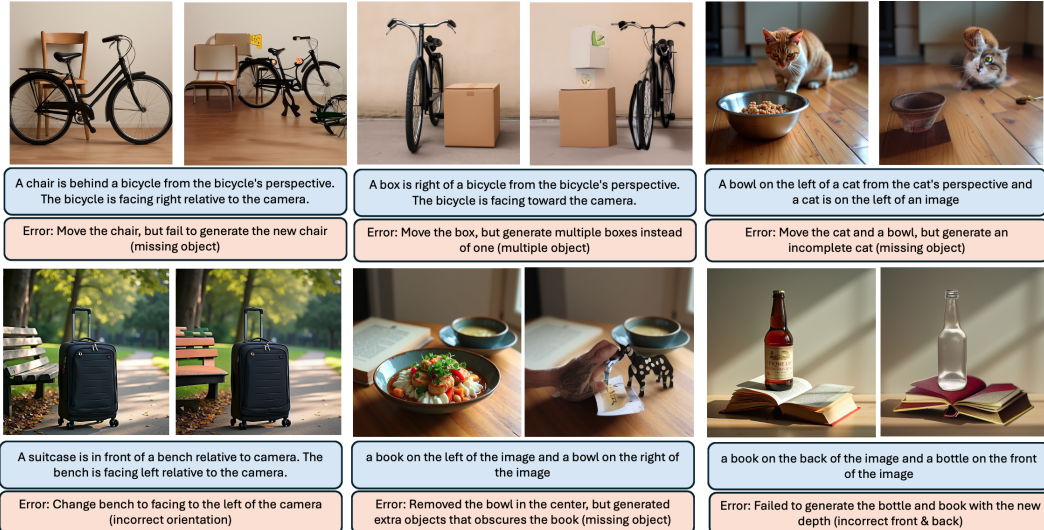


Figure 6: Examples of editing errors using FoR-SALE. The blue box indicates the input spatial expression, while the orange box explains the editing action and the underlying reason for the error.

586 grounding and a more accurate object count. It also shows lower error rates in front/back relations  
 587 and orientation, suggesting improved performance in handling 3D spatial configurations, including  
 588 depth and facing direction. However, GPT-4o performs worse on left/right relations compared to  
 589 the diffusion-based models. We anticipate that this may be attributed to challenges in perspective  
 590 conversion, as evidenced by GPT-4o’s high performance on relative FoRs in the FoR-LMD benchmark  
 591 (94.76%), which requires only camera-centric understanding, contrasted with its significantly lower  
 592 accuracy on intrinsic FoRs, as reported in the main results. These findings suggest a trade-off in  
 593 GPT-4o’s spatial performance—namely, strong handling of camera-centric spatial expressions, but  
 594 limited generalization to non-camera perspectives in text-to-image tasks.

## 595 E Analysis of FoR-SALE framework

### 596 E.1 Additional error analysis of round 1 using initial image from FLUX.1

597 We compare SLD and FoR-SALE in editing images containing front/back spatial relation errors in  
 598 Figure 7. We observe that while SLD attempts to correct the front/back relation, it often introduces  
 599 multiple instances of the target objects instead of editing the original ones. This behavior results in a  
 600 lower front/back error after one round of editing, but it comes at the cost of generating additional  
 601 object-related errors. We attribute this limitation to SLD’s lack of depth awareness, which leads  
 602 to incorrect editing operations. In contrast, FoR-SALE, which incorporates depth information,  
 603 achieves slightly better correction on front/back errors without introducing new object duplication or  
 604 misalignment. Importantly, FoR-SALE avoids introducing new error types, making it more robust for  
 605 subsequent editing rounds.

606 **E.2 Detail Analysis of the effect of different Layout Interpreters and editing actions**

607 We report the distribution of editing actions re-  
 608 quired for images generated by GPT-4o when  
 609 using different Layout Interpreters in Table 5.  
 610 We observe that o3 requires significantly more  
 611 editing actions compared to other models, with  
 612 repositioning accounting for 59.37% of all ac-  
 613 tions (repositioning and depth modification with  
 614 repositioning). This suggests that o3 often gen-  
 615 erates layouts where the object is repositioned,  
 616 likely indicating that it is proposing an entirely  
 617 new scene layout rather than minimally adjust-  
 618 ing the original. This behavior may explain  
 619 the performance drop observed when using o3-  
 620 generated layouts, as reported in the main results.  
 621 It also highlights a limitation of the FoR-SALE  
 622 framework, the difficulty in handling cases that  
 623 require multiple or complex repositioning ac-  
 624 tions. These findings suggest that future work  
 625 may explore improved strategies for accurately  
 626 moving objects—or even fully regenerating im-  
 627 ages—when layout revisions are extensive.

628 **E.3 Examples of failure cases**

629 We present examples of FoR-SALE editing fail-  
 630 ures in Figure 6. The most common errors in-  
 631 clude multiple instances of key objects, incor-  
 632 rect orientation, and missing objects, as also  
 633 reflected in the main paper’s quantitative results. We anticipate these failures primarily to challenges  
 634 in object removal and re-generation, which can lead to either the unintended deletion of key objects or  
 635 the generation of extraneous ones—ultimately making the intended objects undetectable in the final  
 636 image. Additionally, we believe that modifying orientation and depth remains difficult for current  
 637 diffusion models, which limits the effectiveness of FoR-SALE in correcting these types of spatial  
 638 errors.

639 **F Perspective Conversion Rules**

640 In this section, we present all perspective conversion rules used in the FoR Interpreter and the  
 641 corresponding evaluation method. The rules are categorized by the facing direction of the reference  
 642 object. Each facing direction is associated with exactly four conversion rules, corresponding to the  
 643 four spatial relations considered in this work, i.e., left, right, front, and back.

644 [label=0.]Facing toward the camera.

- 645 1. (a) Left. If the object is facing toward the camera (front), then the left side of the object is  
 646 on the right from the camera perspective.
- 647 (b) Right. If the object is facing toward the camera (front), then the right side of the object  
 648 is on the left from the camera perspective.
- 649 (c) Front. If the object is facing toward the camera (front), then the front side of the object  
 650 is in the front direction from the camera perspective.
- 651 (d) Back. If the object is facing toward the camera (front), then the back side of the object  
 652 is in the back direction from the camera perspective.

- 653 2. Facing forward-left.
- 654 (a) Left. If the object is facing forward-left, then the left side of the object is on the right  
 655 from the camera perspective.
- 656 (b) Right. If the object is facing forward-left, then the right side of the object is on the left  
 657 from the camera perspective.

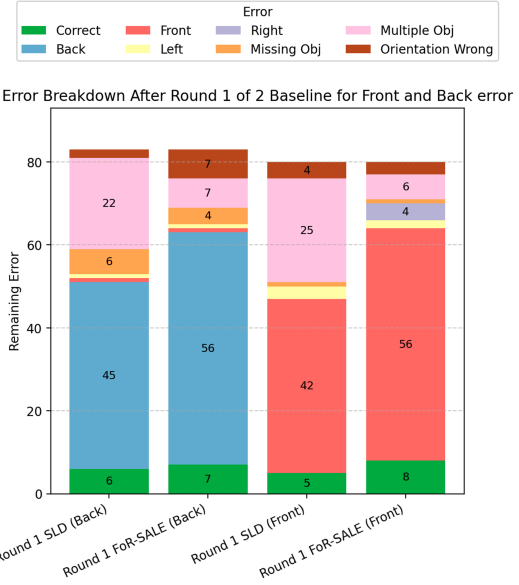


Figure 7: Error breakdown after one round of editing initial images from FLUX.1 using SLD and FoR-SALE on front and back relation errors.

658 (c) Front. If the object is facing forward-left, then the front side of the object is in the front  
659 direction from the camera perspective.  
660 (d) Back. If the object is facing forward-left, then the back side of the object is in the back  
661 direction from the camera perspective.

662 3. Facing left.  
663 (a) Left. If the object is facing left, then the left side of the object is in the front direction  
664 from the camera perspective.  
665 (b) Right. If the object is facing left, then the right side of the object is in the back direction  
666 from the camera perspective.  
667 (c) Front. If the object is facing left, then the front side of the object is on the left from the  
668 camera perspective.  
669 (d) Back. If the object is facing left, then the back side of the object is on the right from  
670 the camera perspective.

671 4. Facing backward-left.  
672 (a) Left. If the object is facing backward-left, then the left side of the object is on the left  
673 from the camera perspective.  
674 (b) Right. If the object is facing backward-left, then the right side of the object is on the  
675 right from the camera perspective.  
676 (c) Front. If the object is facing backward-left, then the front side of the object is in the  
677 back direction from the camera perspective.  
678 (d) Back. If the object is facing backward-left, then the back side of the object is in the  
679 front direction from the camera perspective.

680 5. Facing away from the camera.  
681 (a) Left. If the object is facing away from the camera (back), then the left side of the object  
682 is on the left from the camera perspective.  
683 (b) Right. If the object is facing away from the camera (back), then the right side of the  
684 object is on the right from the camera perspective.  
685 (c) Front. If the object is facing away from the camera (back), then the front side of the  
686 object is in the back direction from the camera perspective.  
687 (d) Back. If the object is facing away from the camera (back), then the back side of the  
688 object is in the front direction from the camera perspective.

689 6. Facing backward-right.  
690 (a) Left. If the object is facing backward-right, then the left side of the object is on the left  
691 from the camera perspective.  
692 (b) Right. If the object is facing backward-right, then the right side of the object is on the  
693 right from the camera perspective.  
694 (c) Front. If the object is facing backward-right, then the front side of the object is in the  
695 back direction from the camera perspective.  
696 (d) Back. If the object is facing backward-right, then the back side of the object is in the  
697 front direction from the camera perspective.

698 7. Facing right.  
699 (a) Left. If the object is facing right, then the left side of the object is in the back direction  
700 from the camera perspective.  
701 (b) Right. If the object is facing right, then the right side of the object is in the front  
702 direction from the camera perspective.  
703 (c) Front. If the object is facing right, then the front side of the object is on the right from  
704 the camera perspective.  
705 (d) Back. If the object is facing right, then the back side of the object is on the left from  
706 the camera perspective.

707 8. Facing forward-right.  
708 (a) Left. If the object is facing forward-right, then the left side of the object is on the right  
709 from the camera perspective.

710 (b) Right. If the object is facing forward-right, then the right side of the object is on the  
 711 left from the camera perspective.  
 712 (c) Front. If the object is facing forward-right, then the front side of the object is in the  
 713 front direction from the camera perspective.  
 714 (d) Back. If the object is facing forward-right, then the back side of the object is in the  
 715 back direction from the camera perspective.

716 **G LLM Prompts**

717 We provide the prompt for LLM used throughout the entire experiments in this section.

Listing 1: Prompt for generate layout for GLIGEN.

```
718 Your task is to generate the bounding boxes of objects mentioned in
719 the caption, along with direction that objects facing.
720 The image is size 512x512.
721 The bounding box should be in the format of (x, y, width, height) from
722 0 to 1.
723 The direction that object is facing should be one of these options, [front,
724 back, left, right]
725 Please considering the frame of reference of caption and direction of
726 reference object.
727 The answer should be in the form of "Reasoning: Explanation\nLayout:
728 Layout\" The example of layout is [(cat, [0.1, 0.3, 0.5, 0.4],
729 right), (cow, [0.6, 0.5, 0.3, 0.4], right)]"
```

Listing 2: Prompt for LLM Parser.

```
732 # Your Role: Excellent Parser
733
734 ## Objective: Analyze scene descriptions to identify objects and their
735 attributes.
736
737 ## Process Steps
738 1. Read the user prompt (scene description).
739 2. Identify all objects mentioned with quantities.
740 3. Extract attributes of each object (color, size, material, etc.).
741 4. Ignore facing attribute (facing to left, facing to right, facing
742 forward)
743 5. If the description mentions objects that shouldn't be in the image,
744 take note at the negation part.
745 6. Explain your understanding (reasoning) and then format your result
746 (answer / negation) as shown in the examples.
747 7. Importance of Extracting Attributes: Attributes provide specific
748 details about the objects. This helps differentiate between
749 similar objects and gives a clearer understanding of the scene.
750
751 ## Examples
752
753 - Example 1
754   User prompt: A brown horse is beneath a black dog. Another orange
755   cat is beneath a brown horse.
756   Reasoning: The description talks about three objects: a brown
757   horse, a black dog, and an orange cat. We report the color
758   attribute thoroughly. No specified negation terms. No
759   background is mentioned and thus fill in the default one.
760   Objects: [('horse', ['brown']), ('dog', ['black']), ('cat', [
761     'orange'])]
762   Background: A realistic image
763   Negation:
764
765 - Example 2
766   User prompt: There's a white car and a yellow airplane in a garage
767   . They're in front of two dogs and behind a cat. The car is
768   small. Another yellow car is outside the garage.
```

```

770 Reasoning: The scene has two cars, one airplane, two dogs, and a
771 cat. The car and airplane have colors. The first car also has
772 a size. No specified negation terms. The background is a
773 garage.
774 Objects: [('car', ['white and small', 'yellow']), ('airplane', [
775     'yellow']), ('dog', [None, None]), ('cat', [None])]
776 Background: A realistic image in a garage
777 Negation:
778
779 - Example 3
780     User prompt: A car and a dog are on top of an airplane and below a
781     red chair. There's another dog sitting on the mentioned chair
782 .
783     Reasoning: Four objects are described: one car, airplane, two dog,
784     and a chair. The chair is red color. No specified negation
785     terms. No background is mentioned and thus fill in the default
786     one.
787     Objects: [('car', [None]), ('airplane', [None]), ('dog', [None,
788         None]), ('chair', ['red'])]
789     Background: A realistic image
790     Negation:
791
792 - Example 4
793     User prompt: An oil painting at the beach of a blue bicycle to the
794     left of a bench and to the right of a palm tree with five
795     seagulls in the sky.
796     Reasoning: Here, there are five seagulls, one blue bicycle, one
797     palm tree, and one bench. No specified negation terms. The
798     background is an oil painting at the beach.
799     Objects: [('bicycle', ['blue']), ('palm tree', [None]), ('seagull',
800         , [None, None, None, None, None]), ('bench', [None])]
801     Background: An oil painting at the beach
802     Negation:
803
804 - Example 5
805     User prompt: An animated-style image of a scene without backpacks.
806     Reasoning: The description clearly states no backpacks, so this
807     must be acknowledged. The user provides the negative prompt of
808     backpacks. The background is an animated-style image.
809     Objects: [('backpacks', [None])]
810     Background: An animated-style image
811     Negation: backpacks
812
813 - Example 6
814     User Prompt: Make the dog a sleeping dog and remove all shadows in
815     an image of a grassland.
816     Reasoning: The user prompt specifies a sleeping dog on the image
817     and a shadow to be removed. The background is a realistic
818     image of a grassland.
819     Objects: [('dog', ['sleeping']), ['shadow', [None]]]
820     Background: A realistic image of a grassland
821     Negation: shadows
822
823 - Example 7
824     User Prompt: A fire hydrant is back of a cat relative to observer.
825     The cat is facing away from the observer.
826     Reasoning: Two objects are described: one fire hydrant, and a cat.
827     No specified negation terms. No background is mentioned and
828     thus fill in the default one.
829     Objects: [('fire hydrant', [None]), ['cat', [None]]]
830     Background: A realistic image
831     Negation: shadows
832

```

```

833 | Your Current Task: Follow the steps closely and accurately identify
834 | objects based on the given prompt. Ensure adherence to the above
835 | output format.
836 |

```

Listing 3: Prompt for FoR Interpreter.

```

837 #
838 # Your Role: Expert on spatial relation in multiple perspectives
839
840 ## Objective: Interpret the prompt and convert the spatial relation
841     into the camera's perspective
842
843 ## Image and Object Specification
844 1. Image Coordinates: Define square images with top-left at [0, 0] and
845     bottom-right at [1, 1].
846 2. Four of the information objects are given in order, object name,
847     bounding box, depth, and facing direction
848 3. Object Format: (object, box, depth, facing direction)
849 4. Box Format: [Top-left x, Top-left y, Width, Height]
850 5. Depth: Define depth of the object from furthest at 0 and nearest at
851     1.
852 6. Facing Direction: An orientation of the object relative to the
853     camera which can be None, left, forward-left, backward-left, right
854     , forward-right, backward-right, front (facing forward or facing
855     toward), or back (facing backward or facing away).
856
857 ## Key Guidelines
858 1. Perspective Identification: Carefully consider the perspective of
859     the spatial relation presented in the prompt.
860 2. Object facing direction: Carefully consider the facing orientation
861     presented in the prompt first, before considering the facing
862     orientation from the object specification.
863 3. Assume the camera, observer, and I (me) are the same thing and have
864     the same view (perspective).
865 4. Look at the example closely to see how the conversion need to make.
866 <RULES>
867
868 ## Process Steps
869 1. Read and understand the user prompt (scene description).
870 2. Identify the perspective of the spatial relation presented in the
871     given prompt.
872 2. Check whether the facing direction is provided in the prompt.
873 3. If not, check the facing direction presented in the object
874     specification.
875 4. Explain your understanding (reasoning) and then convert the
876     perspective into the camera's perspective
877 5. If there is no specification of perspective, assume the camera
878     perspective for minimal editing of the given prompt.
879 6. Do not modify other part of the prompt except for spatial relation(
880     s).
881 7. Do not update the object, only modify the prompt.
882
883 ## Examples
884
885 - Example 1
886     User prompt: a backpack on the right of a car from car's
887         perspective and a car on the left
888     Current Objects: [('backpack #1', [0.302, 0.293, 0.335, 0.194],
889         0.63, None), ('car #1', [0.027, 0.324, 0.246, 0.160]), 0.25, "
890         left"]
891     Reasoning: There are two spatial relations presented in the prompt
892         . The first one specifies a backpack on the right of a car
893         from "the car's perspective." There is no specific the facing
894         direction of the car presented in the prompt. Therefore,
895         consider the car's facing direction in the object's current
896         state ("left"). The car is facing to the left of the photo.
897

```

```

898 Therefore, the right of the car from "car's perspective" is
899 back of the camera. Then, the first spatial relation in the
900 camera's perspective is that the backpack is back of the car
901 from the camera's perspective. The second spatial relation is
902 a car on the left. This does not specify the perspective. Then
903 , assuming a camera perspective for this one. Therefore, no
904 update for the second spatial relation.
905 Updated prompt: a backpack on the back of a car from camera's
906 perspective and a car on the left
907
908 - Example 2
909 User prompt: a cat is on the left and the cup is on the right of
910 the cat from the cat's view
911 Current Objects: [('cat #1', [0.169, 0.563, 0.323, 0.291], 0.901,
912 'right'), ('cup #1', [0.59, 0.186, 0.408, 0.814], 0.732, None)
913 ]
914 Reasoning: There are two spatial relations presented in the prompt
915 . The first spatial relation is a cat on the left. The prompt
916 does not specify the perspective. Then, assuming a camera
917 perspective for this one. Therefore, no update for the first
918 spatial relation. The second one specifies the cup is on the
919 right of the cat from "the cat's view." There is no specific
920 direction facing the cat in the present in the prompt.
921 Therefore, consider the cat's facing direction in the object's
922 current state ("right"). The cat is facing to the right of
923 the photo. Therefore, the right of the cat from "cat's
924 perspective" is front of the camera. Then, the second spatial
925 relation in the camera's perspective is that the cup on the
926 front of the cat from the camera's view.
927 Updated prompt: a cat is on the left and the cup is on the front
928 of the cat from the camera's view
929
930 - Example 3
931 User prompt: A cow is in front of a sheep from the camera angle.
932 The sheep is facing right relative to the camera.
933 Current Objects: [('cow #1', [0.354, 0.365, 0.285, 0.385], 0.41,
934 'None'), ('sheep #1', [0.608, 0.120, 0.285, 0.200], 0.82,
935 "right")]
936 Reasoning: There is only one spatial relation presented in the
937 prompt. The prompt specifies that a cow is in front of a sheep
938 from the "camera angle." This spatial relation is from the
939 camera's perspective. Therefore, there is no need for change.
940 Updated prompt: A cow is in front of a sheep from the camera angle
941 . The sheep is facing right relative to the camera.
942
943 - Example 4
944 User prompt: A fire hydrant is back of a sheep from the sheep's
945 perspective. The sheep is facing away from the camera.
946 Current Objects: [('fire hydrant #1', [0.113, 0.365, 0.251,
947 0.251], 0.64, None), ('sheep #1', [0.608, 0.120, 0.251,
948 0.251], 0.52, "back")]
949 Reasoning: There is only one spatial relation presented in the
950 prompt. The prompt specifies that a fire hydrant is back of a
951 sheep from "the sheep's perspective." The prompt also
952 specifies that the sheep is facing away (back) from the camera
953 . So, the back of the sheep is the front direction of the
954 camera. The updated spatial prompt is a fire hydrant is front
955 of a sheep from the camera's perspective.
956 Updated prompt: A fire hydrant is front of a sheep from the camera
957 's perspective. The sheep is facing away from the camera.
958
959 - Example 5
960 User prompt: A deer is to the left of a car from the car's
961 perspective. The car is facing away from the camera.

```

```

962     Current Objects: [('deer #1', [0.454, 0.165, 0.285, 0.385], 0.42,
963         None), ('car #1', [0.608, 0.620, 0.285, 0.200], 0.83, "back")]
964     Reasoning: There is only one spatial relation presented in the
965         prompt. The prompt specifies that a deer is to the left of a
966         car from "the car's perspective." The prompt also specifies
967         that the car is facing away (back) from the camera. So, the
968         left side of the car that is facing away is the left direction
969         of the camera. The updated spatial prompt is a deer is to the
970         left of a car from the camera's perspective.
971     Updated prompt: A deer is to the left of a car from the camera's
972         perspective. The car is facing away from the camera.
973
974 - Example 6
975     User prompt: A cow is to the right of a horse from the horse's
976         perspective. The horse is facing toward relative to the camera
977         .
978     Current Objects: [('Cow #1', [0.113, 0.365, 0.352, 0.352], 0.83,
979         None), ('horse #1', [0.608, 0.120, 0.352, 0.352], 0.25, "front
980        ")]
981     Reasoning: There is only one spatial relation presented in the
982         prompt. The prompt specifies that a cow is to the right of a
983         horse from "the horse's perspective." The prompt also
984         specifies that the horse is facing toward (front) the camera.
985         So, the right of the horse facing toward is the left direction
986         of the camera. The updated spatial prompt is a cow is to the
987         left of a horse from the camera's perspective.
988     Updated prompt: A cow is to the left of a horse from the camera's
989         perspective. The horse is facing toward relative to the camera
990         .
991
992 - Example 7
993     User prompt: A deer is in front of a sheep from the sheep's
994         perspective. The sheep is facing toward relative to the camera
995         .
996     Current Objects: [('deer #1', [0.454, 0.365, 0.285, 0.385], 0.64,
997         None), ('sheep #1', [0.608, 0.120, 0.285, 0.200], 0.32, "front
998        ")]
999     Reasoning: There is only one spatial relation presented in the
1000         prompt. The prompt specifies that a deer is in front of a sheep
1001         from "the sheep's perspective." The prompt also specifies that
1002         the sheep is facing toward (front) the camera. So, the front
1003         of the sheep that faces toward is the front direction of the
1004         camera. The updated spatial prompt is a deer is in front of a
1005         sheep from the camera's perspective.
1006     Updated prompt: A deer is in front of a sheep from the camera's
1007         perspective. The sheep is facing toward relative to the camera
1008         .
1009
1010 - Example 8
1011     User prompt: A deer is in front of a dog from the dog's
1012         perspective. The dog is facing right relative to the camera.
1013     Current Objects: [('deer #1', [0.186, 0.592, 0.449, 0.408], 0.45,
1014         "front"), ('dog #1', [0.376, 0.194, 0.624, 0.502], 0.53, "
1015         right")]
1016     Reasoning: There is only one spatial relation presented in the
1017         prompt. The prompt specifies that a deer is in front of a dog
1018         from "the dog's perspective." The prompt also specifies that
1019         the dog is facing to the right of the camera. So, the front of
1020         the dog that is facing right is the right direction of the
1021         camera. The updated spatial prompt is a deer is to the right
1022         of a dog from the camera's perspective.
1023     Updated prompt: A deer is to the right of a dog from the camera's
1024         perspective. The dog is facing right relative to the camera.
1025
1026 - Example 9

```

```

1027 User prompt: A deer is to the right of a car from the car's
1028 perspective. The car is facing away from the camera.
1029 Current Objects: [('deer #1', [0.454, 0.165, 0.285, 0.385], 0.42,
1030 None), ('car #1', [0.608, 0.620, 0.285, 0.200], 0.83, "back")]
1031 Reasoning: There is only one spatial relation presented in the
1032 prompt. The prompt specifies that a deer is to the right of a
1033 car from "the car's perspective." The prompt also specifies
1034 that the car is facing away (back) from the camera. So, the
1035 right side of the car that is facing away is the right
1036 direction of the camera, don't reverse the literal relation
1037 like facing toward the camera. The updated spatial prompt is
1038 that a deer is to the right of a car from the camera's
1039 perspective.
1040 Updated prompt: A deer is to the right of a car from the camera's
1041 perspective. The car is facing away from the camera.
1042
1043 Your Current Task: Follow the steps closely and accurately convert all
1044 presented spatial relations in the given prompt into the camera's
1045 perspective. Ensure adherence to the above output format.

```

Listing 4: Prompt for Layout Interpreter.

```

1047 # Your Role: Expert Bounding Box Adjuster
1048
1049 ## Objective: Manipulate bounding boxes in square images according to
1050 the user prompt while maintaining visual accuracy.
1051
1052 ## Object Specifications and Manipulations
1053 1. Image Coordinates: Define square images with top-left at [0, 0] and
1054 bottom-right at [1, 1].
1055 2. Object Format: (object, box, depth, orientation)
1056 3. Box Format: [Top-left x, Top-left y, Width, Height]
1057 4. Depth: Define depth of the object from furthest at 0 and nearest at
1058 1.
1059 5. Orientation Format: An orientation of the object which can be None,
1060 Left, Right, Front, or Back.
1061 6. Operations: Include addition, deletion, repositioning, attribute
1062 modification, and depth modification.
1063
1064 ## Key Guidelines
1065 1. Alignment: Follow the user's prompt, keeping the specified object
1066 count and attributes. Deem it incorrect if the
1067 described object lacks specified attributes.
1068 2. Boundary Adherence: Keep bounding box coordinates within [0, 1].
1069 3. Depth Adherence: Keep average depth within [0, 1].
1070 4. Orientation Adherence: An orientation must change depend on the
1071 prompt. If nothing specify in the prompt, do not change the
1072 orientation of the object.
1073 5. Minimal Modifications: Change bounding boxes or depth only if they
1074 don't match the user's prompt (i.e., don't modify matched objects)
1075 .
1076 6. Overlap Reduction: Minimize intersections in new boxes and remove
1077 the smallest, least overlapping objects.
1078
1079 ## Process Steps
1080 1. Interpret prompts: Read and understand the user's prompt.
1081 2. Implement Changes: Review and adjust current bounding boxes to meet
1082 user specifications.
1083 3. Explain Adjustments: Justify the reasons behind each alteration and
1084 ensure every adjustment abides by the key guidelines.
1085 4. Output the Result: Present the reasoning first, followed by the
1086 updated objects section, which should include a list of bounding
1087 boxes in Python format.
1088
1089 ## Examples
1090
1091

```

```

1092 - Example 1
1093     User prompt: A realistic image of landscape scene depicting a
1094         green car parking on the left of a blue truck, with a red air
1095         balloon and a bird in the sky
1096     Current Objects: [('green car #1', [0.027, 0.365, 0.275, 0.207],
1097         0.6, None), ('blue truck #1', [0.350, 0.368, 0.272, 0.208],
1098         0.7, None), ('red air balloon #1', [0.086, 0.010, 0.189,
1099         0.176]), 0.4, None]
1100     Reasoning: To add a bird in the sky as per the prompt, ensuring
1101         all coordinates and dimensions remain within [0, 1].
1102     Updated Objects: [('green car #1', [0.027, 0.365, 0.275, 0.207],
1103         0.6, None), ('blue truck #1', [0.350, 0.369, 0.272, 0.208],
1104         0.7, None), ('red air balloon #1', [0.086, 0.010, 0.189,
1105         0.176]), 0.4, None), ('bird #1', [0.385, 0.054, 0.186, 0.130]),
1106         0.3, None]
1107
1108 - Example 2
1109     User prompt: A realistic image of landscape scene depicting a
1110         green car parking on the right of a blue truck, with a red air
1111         balloon and a bird in the sky
1112     Current Output Objects: [('green car #1', [0.027, 0.365, 0.275,
1113         0.207], 0.79, "left"), ('blue truck #1', [0.350, 0.369, 0.272,
1114         0.208], 0.68, "right"), ('red air balloon #1', [0.086, 0.010,
1115         0.189, 0.176]), 0.15, None]
1116     Reasoning: The relative positions of the green car and blue truck
1117         do not match the prompt. Swap positions of the green car and
1118         blue truck to match the prompt, while keeping all coordinates
1119         and dimensions within [0, 1].
1120     Updated Objects: [('green car #1', [0.350, 0.369, 0.275, 0.207],
1121         0.79, "left"), ('blue truck #1', [0.027, 0.365, 0.272, 0.208],
1122         0.68, "right"), ('red air balloon #1', [0.086, 0.010, 0.189,
1123         0.176]), 0.15, None), ('bird #1', [0.485, 0.054, 0.186, 0.130],
1124         0.15, "front")]
1125
1126 - Example 3
1127     User prompt: An oil painting of a pink dolphin jumping on the left
1128         of a steam boat on the sea
1129     Current Objects: [('steam boat #1', [0.302, 0.293, 0.335, 0.194],
1130         0.76, "front"), ('pink dolphin #1', [0.027, 0.324, 0.246,
1131         0.160], 0.23, "left"), ('blue dolphin #1', [0.158, 0.454,
1132         0.376, 0.290], 0.26, "right")]
1133     Reasoning: The prompt mentions only one dolphin, but two are
1134         present. Thus, remove one dolphin to match the prompt,
1135         ensuring all coordinates and dimensions stay within [0, 1].
1136     Updated Objects: [('steam boat #1', [0.302, 0.293, 0.335, 0.194],
1137         0.76, "front"), ('pink dolphin #1', [0.027, 0.324, 0.246,
1138         0.160], 0.23, "left")]
1139
1140 - Example 4
1141     User prompt: An oil painting of a pink dolphin jumping on the left
1142         of a steam boat on the sea
1143     Current Objects: [('steam boat #1', [0.302, 0.293, 0.335, 0.194],
1144         0.76, "front"), ('dolphin #1', [0.027, 0.324, 0.246, 0.160],
1145         0.23, "left")]
1146     Reasoning: The prompt specifies a pink dolphin, but there's only a
1147         generic one. The attribute needs to be changed.
1148     Updated Objects: [('steam boat #1', [0.302, 0.293, 0.335, 0.194],
1149         0.76, "front")), ('pink dolphin #1', [0.027, 0.324, 0.246,
1150         0.160], 0.23, "left")]
1151
1152 - Example 5
1153     User prompt: a backpack on the right of a car from car's
1154         perspective and a car on the left

```

```

1155 Current Objects: [('backpack #1', [0.302, 0.293, 0.335, 0.194],  

1156 0.63, None), ('car #1', [0.027, 0.324, 0.246, 0.160]), 0.25, "  

1157 left"]  

1158 Reasoning: The prompt specifies that a backpack on the right of "a  

1159 car". There is no specific of orientation of the car from the  

1160 prompt, however, the current car is facing to the left.  

1161 Therefore, the spatial relation from the camera should be that  

1162 a backpack on the back of the car. Average depth of backpack  

1163 (0.63) is higher than a car(0.25) which do not match the  

1164 prompt. Swap the average depth of the car and the backpack to  

1165 match the prompt, while keeping all coordinates and dimensions  

1166 within [0, 1].  

1167 Updated Objects: [('backpack #1', [0.302, 0.293, 0.335, 0.194],  

1168 0.25, None), ('car #1', [0.027, 0.324, 0.246, 0.160]), 0.63, "  

1169 left"]  

1170  

1171 - Example 6  

1172 User prompt: a cat is on the left and the cup is on the right of  

1173 the cat from the cat's view  

1174 Current Objects: [('cat #1', [0.169, 0.563, 0.323, 0.291], 0.901,  

1175 'right'), ('cup #1', [0.59, 0.186, 0.408, 0.814], 0.732, None)  

1176 ]  

1177 Reasoning: The prompt specifies that a cat is on the left, which  

1178 is currently correct. There is no specific of cat's  

1179 orientation in the prompt. Then, the right orientation is  

1180 acceptable. Then, the prompt specifies that a cup is to the  

1181 right of cat the cat's view. This is same as a cup is in front  

1182 of the cat from camera's perspective. However, cup's depth  

1183 (0.731) is lower than cat's depth (0.901). Considering only  

1184 increasing cup's depth and lowering cat's depth, while keeping  

1185 all coordinates and dimension within [0, 1].  

1186 Updated Objects: [('cat #1', [0.169, 0.563, 0.323, 0.291], 0.405,  

1187 'right'), ('cup #1', [0.59, 0.186, 0.408, 0.814], 0.901, None)  

1188 ]  

1189  

1190 - Example 7  

1191 User prompt: A cow is in front of a sheep from the camera angle.  

1192 The sheep is facing right relative to the camera.  

1193 Current Objects: [('cow #1', [0.354, 0.365, 0.285, 0.385], 0.41, "  

1194 None"), ('sheep #1', [0.608, 0.120, 0.285, 0.200], 0.82, "  

1195 right")]  

1196 Reasoning: The prompt specifies that a cow is in front of a sheep  

1197 from "the camera angle". Therefore, the spatial relation is  

1198 that a cow is in front of a sheep from the camera's  

1199 perspective. However, the depth of the cow is lower than the  

1200 sheep, which does not match the prompt. Swap the average depth  

1201 of the cow and the sheep to match the prompt, while keeping  

1202 all coordinates and dimensions within [0, 1].  

1203 Updated Objects: [('cow #1', [0.354, 0.365, 0.285, 0.385], 0.82,  

1204 "None"), ('sheep #1', [0.608, 0.120, 0.285, 0.200], 0.41, "  

1205 right")]  

1206  

1207 - Example 8  

1208 User prompt: A fire hydrant is back of a sheep from the sheep's  

1209 perspective. The sheep is facing left relative to the camera.  

1210 Current Objects: [('fire hydrant #1', [0.113, 0.365, 0.251,  

1211 0.251], 0.64, None), ('sheep #1', [0.608, 0.120, 0.251,  

1212 0.251], 0.52, "left")]  

1213 Reasoning: The prompt specifies that a fire hydrant is back of a  

1214 sheep from "the sheep's perspective". Since the sheep is  

1215 facing to the left of the camera from the prompt, the spatial  

1216 relation from the camera should be that a fire hydrant is  

1217 right of the sheep from the camera's perspective. Therefore,  

1218 the relative positions of the fire hydrant and sheep do not  

1219 match the prompt since the fire hydrant's bounding box is to

```

```

1220     the left of the sheep's bounding box. Swap positions of the
1221     fire hydrant and sheep to match the prompt, while keeping all
1222     coordinates and dimensions within [0, 1].
1223     Updated Objects:[('fire hydrant #1', [0.608, 0.120, 0.251, 0.251],
1224     0.64, None), ('sheep #1', [0.113, 0.365, 0.251, 0.251], 0.52,
1225     "left")]
1226
1227 - Example 9
1228     User prompt: A cow is to the left of a horse from the horse's
1229     perspective. The horse is facing right relative to the camera.
1230     Current Objects: [('Cow #1', [0.113, 0.365, 0.352, 0.352], 0.83,
1231     None), ('horse #1', [0.608, 0.120, 0.352, 0.352], 0.25, "right
1232     ")]
1233     Reasoning: The prompt specifies that a cow is to the left of a
1234     horse from "the horse's perspective". Since the horse is
1235     facing to the right of the camera from the prompt, the spatial
1236     relation from the camera should be that a cow is back of a
1237     horse from the camera's perspective. However, the depth of the
1238     cow (0.83) is higher than the horse (0.25), which does not
1239     match the prompt. Swap the average depth of the cow and the
1240     horse to match the prompt, while keeping all coordinates and
1241     dimensions within [0, 1].
1242     Updated Objects: [('Cow #1', [0.113, 0.365, 0.352, 0.352], 0.25,
1243     None), ('horse #1', [0.608, 0.120, 0.352, 0.352], 0.83, "right
1244     ")]
1245
1246 - Example 10
1247     User prompt: A deer is in front of a car from the car's
1248     perspective. The car is facing toward the camera.
1249     Current Objects: [('deer #1', [0.454, 0.365, 0.285, 0.385], 0.64,
1250     None), ('car #1', [0.608, 0.120, 0.285, 0.200], 0.32, "left")]
1251     Reasoning: The prompt specifies that a deer is in front of a car
1252     from "the car's perspective". Since the car is facing toward
1253     the camera from the prompt, the spatial relation from the
1254     camera should be that a deer is in front of a car from the
1255     camera's perspective. Average depth of deer (0.64) is higher
1256     than average depth of cow (0.32), match the prompt. However,
1257     the orientation of the car is left. The orientation of car
1258     need to be changed.
1259     Updated Objects: [('deer #1', [0.454, 0.365, 0.285, 0.385], 0.64,
1260     None), ('car #1', [0.608, 0.120, 0.285, 0.200], 0.32, "front
1261     ")]
1262
1263 - Example 11
1264     User prompt: A deer is in front of a car from the car's
1265     perspective. The car is facing away from the camera.
1266     Current Objects: [('deer #1', [0.454, 0.165, 0.285, 0.385], 0.42,
1267     None), ('car #1', [0.608, 0.620, 0.285, 0.200], 0.83, "back")]
1268     Reasoning: The prompt specifies that a deer is in front of a car
1269     from "the car's perspective". Since the car is facing away
1270     from the camera from the prompt, the spatial relation from the
1271     camera should be that a deer is back of a car from the camera
1272     's perspective. Average depth of deer is lower than average
1273     depth of cow. Thus, the image aligns with the user's prompt,
1274     requiring no further modifications.
1275     Updated Objects: [('deer #1', [0.454, 0.165, 0.285, 0.385], 0.42,
1276     None), ('car #1', [0.608, 0.620, 0.285, 0.200], 0.83, "back")]
1277
1278 - Example 12
1279     User prompt: A realistic photo of a scene with a brown bowl on the
1280     right and a gray dog on the left
1281     Current Objects: [('gray dog #1', [0.186, 0.592, 0.449, 0.408],
1282     0.45, "front"), ('brown bowl #1', [0.376, 0.194, 0.624,
1283     0.502], 0.53, None)]

```

```
1284 Reasoning: The leftmost coordinate (0.186) of the gray dog's
1285 bounding box is positioned to the left of the leftmost
1286 coordinate (0.376) of the brown bowl, while the rightmost
1287 coordinate (0.186 + 0.449) of the bounding box has not
1288 extended beyond the rightmost coordinate of the bowl. Thus,
1289 the image aligns with the user's prompt, requiring no further
1290 modifications.
1291 Updated Objects: [('gray dog #1', [0.186, 0.592, 0.449, 0.408],
1292 0.45, "front"), ('brown bowl #1', [0.376, 0.194, 0.624,
1293 0.502], 0.53, None)]
1294
1295 Your Current Task: Carefully follow the provided guidelines and steps
1296 to adjust bounding boxes in accordance with the user's prompt.
1297 Ensure adherence to the above output format.
```

1299 **NeurIPS Paper Checklist**

1300 **1. Claims**

1301 Question: Do the main claims made in the abstract and introduction accurately reflect the  
1302 paper's contributions and scope?

1303 Answer: **[Yes]**

1304 Justification: We provide the experiment results and discussion that support claims made in  
1305 the abstract and introduction.

1306 **2. Limitations**

1307 Question: Does the paper discuss the limitations of the work performed by the authors?

1308 Answer: **[Yes]**

1309 Justification: We have the limitations section in the main content.

1310 **3. Theory assumptions and proofs**

1311 Question: For each theoretical result, does the paper provide the full set of assumptions and  
1312 a complete (and correct) proof?

1313 Answer: **[NA]**

1314 Justification: This paper does not include any theoretical results.

1315 **4. Experimental result reproducibility**

1316 Question: Does the paper fully disclose all the information needed to reproduce the main ex-  
1317 perimental results of the paper to the extent that it affects the main claims and/or conclusions  
1318 of the paper (regardless of whether the code and data are provided or not)?

1319 Answer: **[Yes]**

1320 Justification:

1321 **5. Open access to data and code**

1322 Question: Does the paper provide open access to the data and code, with sufficient instruc-  
1323 tions to faithfully reproduce the main experimental results, as described in supplemental  
1324 material?

1325 Answer: **[Yes]**

1326 Justification: We provide the zip file containing the code for our paper, following the  
1327 NeurIPS guidelines.

1328 **6. Experimental setting/details**

1329 Question: Does the paper specify all the training and test details (e.g., data splits, hyper-  
1330 parameters, how they were chosen, type of optimizer, etc.) necessary to understand the  
1331 results?

1332 Answer: **[Yes]**

1333 Justification: We provide all details of the experiment setting in Section 4 and Appendix A

1334 **7. Experiment statistical significance**

1335 Question: Does the paper report error bars suitably and correctly defined or other appropriate  
1336 information about the statistical significance of the experiments?

1337 Answer: **[No]**

1338 Justification: Our experiment results are not accompanied by error bars, confidence intervals,  
1339 or statistical significance tests.

1340 **8. Experiments compute resources**

1341 Question: For each experiment, does the paper provide sufficient information on the com-  
1342 puter resources (type of compute workers, memory, time of execution) needed to reproduce  
1343 the experiments?

1344 Answer: **[Yes]**

1345 Justification: We provide the detail on compute resources in Section 4.

1346 **9. Code of ethics**

1347 Question: Does the research conducted in the paper conform, in every respect, with the  
1348 NeurIPS Code of Ethics <https://neurips.cc/public/EthicsGuidelines>?

1349 Answer: [Yes]

1350 Justification: We reviewed the NeurIPS Code of Ethics and confirm that our paper adheres  
1351 to its principles.

1352 **10. Broader impacts**

1353 Question: Does the paper discuss both potential positive societal impacts and negative  
1354 societal impacts of the work performed?

1355 Answer: [Yes]

1356 Justification: We discussed this briefly in the Limitations Section.

1357 **11. Safeguards**

1358 Question: Does the paper describe safeguards that have been put in place for responsible  
1359 release of data or models that have a high risk for misuse (e.g., pretrained language models,  
1360 image generators, or scraped datasets)?

1361 Answer: [NA]

1362 Justification: Our proposed pipeline is based on existing models and does not introduce new  
1363 risks beyond the original one.

1364 **12. Licenses for existing assets**

1365 Question: Are the creators or original owners of assets (e.g., code, data, models), used in  
1366 the paper, properly credited and are the license and terms of use explicitly mentioned and  
1367 properly respected?

1368 Answer: [Yes]

1369 Justification: We properly credited and cited all used assets and datasets.

1370 **13. New assets**

1371 Question: Are new assets introduced in the paper well documented and is the documentation  
1372 provided alongside the assets?

1373 Answer: [Yes]

1374 Justification: We provide all details of our proposed pipeline in the main paper and Appendix.

1375 **14. Crowdsourcing and research with human subjects**

1376 Question: For crowdsourcing experiments and research with human subjects, does the paper  
1377 include the full text of instructions given to participants and screenshots, if applicable, as  
1378 well as details about compensation (if any)?

1379 Answer: [NA]

1380 Justification: We do not involve crowdsourcing nor research with human subjects.

1381 **15. Institutional review board (IRB) approvals or equivalent for research with human  
1382 subjects**

1383 Question: Does the paper describe potential risks incurred by study participants, whether  
1384 such risks were disclosed to the subjects, and whether Institutional Review Board (IRB)  
1385 approvals (or an equivalent approval/review based on the requirements of your country or  
1386 institution) were obtained?

1387 Answer: [NA]

1388 Justification: We do not involve crowdsourcing nor research with human subjects.

1389 **16. Declaration of LLM usage**

1390 Question: Does the paper describe the usage of LLMs if it is an important, original, or  
1391 non-standard component of the core methods in this research? Note that if the LLM is used  
1392 only for writing, editing, or formatting purposes and does not impact the core methodology,  
1393 scientific rigorousness, or originality of the research, declaration is not required.

1394

Answer: [\[Yes\]](#)

1395

1396

1397

Justification: We provide detailed instructions on using LLM in our core method in Methodology and Appendix. We also include the prompt used for each LLM component in our method.